JOURNAL OF GEOPHYSICAL RESEARCH, VOL. 113, A08212, doi:10.1029/2007JA012612, 2008

Influence of the convection electric field models on predicted plasmapause positions during magnetic storms

V. Pierrard,[1,3] G. V. Khazanov,[2] J. Cabrera,[3] and J. Lemaire[1,3]

Received 27 June 2007; revised 28 August 2007; accepted 7 March 2008; published 9 August 2008.

[1] In the present work, we determine how three well documented models of the magnetospheric electric field, and two different mechanisms proposed for the formation of the plasmapause influence the radial distance, the shape and the evolution of the plasmapause during the geomagnetic storms of 28 October 2001 and of 17 April 2002. The convection electric field models considered are: McIlwain's E5D electric field model, Volland-Stern's model, and Weimer's statistical model compiled from low-Earth orbit satellite data. The mechanisms for the formation of the plasmapause to be tested are: (1) the MHD theory where the plasmapause should correspond to the last-closed-equipotential (LCE) or last-closed-streamline (LCS), if the E-field distribution is stationary or time-dependent respectively; (2) the interchange mechanism where the plasmapause corresponds to streamlines tangent to a Zero-Parallel-Force surface where the field-aligned plasma distribution becomes convectively unstable during enhancements of the E-field intensity in the nightside local time sector. The results of the different time dependent simulations are compared with concomitant EUV/IMAGE observations when available. The plasmatails or plumes observed after both selected geomagnetic storms are predicted in all simulations and for all E-field models. However, their shapes are quite different depending on the E-field models and the mechanisms that are used. Despite the partial success of the simulations to reproduce plumes during magnetic storms and substorms, there remains a long way to go before the detailed structures observed in the EUV observations during periods of geomagnetic activity can be accounted for very precisely by the existing E-field models. Furthermore, it cannot be excluded that the mechanisms currently identified to explain the formation of ''Carpenter's knee'' during substorm events, will have to be revised or complemented in the cases of geomagnetic storms.

Citation: Pierrard, V., G. V. Khazanov, J. Cabrera, and J. Lemaire (2008), Influence of the convection electric field models on predicted plasmapause positions during magnetic storms, *J. Geophys. Res.*, *113*, A08212, doi:10.1029/2007JA012612.

1. Introduction

[2] The plasmapause position prediction is very important for the scientific community because the plasmasphere interacts with the other regions of the magnetosphere and with the ionosphere. The location of the plasmapause determines for instance where wave-particle interaction processes change the pitch angle and energy spectra of radiation belts (RB) electrons. *Cornwall et al.* [1971] noted that maximum instability of ElectroMagnetic Ion Cyclotron (EMIC) waves generated by ring current (RC) anisotropy should occur just within the plasmapause. They also suggested that pitch angle diffusion of RC ions resonant with the EMIC waves generated within the plasmapause should be important loss process for the RC. Recent global self-consistent RC/EMIC waves modeling by *Khazanov et al.* [2006] conforms this initial study. It was found that global EMIC wave distribution has a highly plasmapause organized structure during the May, 1998 storm period that has been presented in this study. *Khazanov et al.* [2007] also found that plasmaspheric energy deposition to the thermal electrons via Landau EMIC wave damping is very critical to position of plasmapause.

[3] During magnetic storms, under certain conditions, relativistic electrons with energies $\geq$1 MeV can be removed from the outer RB by EMIC wave scattering. Recent calculations suggest that pitch angle scattering via EMIC waves can compete with Dst effect as a mechanism for depleting relativistic electrons from the outer RB zone during the initial and main phases of a magnetic storm [*Summers and Thorne*, 2003; *Albert*, 2003]. So, it becomes more and more obvious that RC and RB populations are very sensitive to the core plasmasphere distribution and specifically to the position of the plasmapause [*Spasojevic et al.*, 2004; *Baker et al.*, 2004].

[4] The position of the plasmapause is determined by the interplay between the corotation and convection electric fields. This statement is very general but it does not really identify and grasp the specific physical mechanism that is

[1]Belgian Institute for Space Aeronomy, Brussels, Belgium.
[2]National Space Science and Technology Center, NASA Marshall Space Flight Center, Huntsville, Alabama, USA.
[3]Center for Space Radiations, Université Catholique de Louvain, Louvain-La-Neuve, Belgium.

0148-0227/08/2007JA012612$09.00

underlying the formation of the plasmapause. The magnetospheric convection electric field, controlled by the solar wind conditions and the level of geomagnetic activity, is a key factor in all existing theories for the formation of the plasmapause. Therefore it is important to have first a reliable magnetospheric electric field model. Since there is no way to determine directly, at each instant of time, the global electric field distribution in the whole magnetosphere, various empirical and mathematical models have been built, tentatively, with various degrees of sophistication. The E-field models used in the present paper are (1) the VSMC model introduced by Volland and Stern [*Volland*, 1973; *Stern*, 1975] and adapted by *Maynard and Chen* [1975], (2) the E5D model derived by *McIlwain* [1986] from ATS5 and ATS6 observations at geosynchronous orbit, and (3) the model of *Weimer* [1996] determined from ionospheric measurements; these empirical electric field models are respectively associated with (1) a centered dipole magnetic field, (2) the M2 magnetic field determined from geosynchroneous measurements, and (3) *Tsyganenko and Stern*'s [1996] magnetic field model determined from various statistical magnetometric in situ measurements. These models will be briefly described in the next section.

[5] In addition to a reliable magnetospheric electric field model, one needs also to have a correct physical theory for the formation of the plasmapause, i.e., a specific physical mechanism that accounts for the observations. Several such mechanisms have been proposed in the past and can be simulated numerically once an E-field model has been adopted.

[6] In the following sections, we use the three E-field models mentioned above, and compare their influence on the dynamics of the plasmasphere during the geomagnetic storm on 28 October 2001. Moreover, for the E5D model, the dynamical evolution of the cold plasma is tracked by using two different categories of simulations to predict the positions of the plasmapause and its deformations at different times precisely when EUV observations are available.

[7] There are other sophisticated models for the magnetospheric electric field distribution: for instance, AMIE developed by *Richmond and Kamide* [1988]. This popular E-field model was obtained from ground-based (magnetometer and radar) and ionospheric (DMSP satellite) data. Although it might be of some interest to use this additional model, it is not completely clear that ionospheric electric field distribution can be directly mapped up into the equatorial region of the magnetosphere where plasmapause knee start to form. Not only is the actual 3D distribution of magnetic field lines not completely guaranteed, but the existence of field-aligned electric potential drops is likely to jeopardize such a field-aligned mapping of ionospheric E-field into the magnetosphere.

[8] In several studies, different convection electric field models have already been compared with observations [*Jordanova et al.*, 2001; *Boonsiriseth et al.*, 2001; *Khazanov et al.*, 2004]. Their influence on the ring current was analyzed in detail by *Chen et al.* [2003]. However, their effects on particles of lower energies (<10 eV) populating the plasmasphere was less well studied, except by *Liemohn et al.* [2004] who compared some electric field models, and their effects on plasmaspheric morphologies; he used (1) a modified McIlwain electric field model, (2) the Weimer model, and (3) as well as another self-consistent electric potential model for the time span of the recovery phase of the 17 April 2002 magnetic storm. These authors found that all these models have certain strengths but also some weaknesses in predicting the observed plasmapause position during this storm. They found especially that the electric field intensity of Weimer's model was a bit too strong in the inner magnetosphere, leading to a too small plasmasphere. Liemohn's modified McIlwain model (which differs from the original E5D model, and was not used with the associated M2 magnetic field model) has a too small electric field intensity around noon, leading to a plasmapause position that does not correspond to the EUV observations on the dayside although a good fit was obtained in the nightside.

[9] In the present work, we also present the results obtained during this magnetic storm of 17 April 2002, but we have focused our attention on another clean and isolated geomagnetic storm: that observed on 28 October 2001. The VSMC, unmodified E5D and Weimer E-field models have been used with the hope to determine which of them might be the most appropriate for this magnetic storm.

[10] It is commonly assumed that the topologies of both the electric field and magnetic field determine the position where the plasmapause is formed at the time of geomagnetic storms and substorms. Postulating that the plasmapause coincides with the last closed equipotential of the magnetospheric electrostatic field distribution as proposed by *Brice* [1967], this led authors to derive an electric field topology from observed plasmapause positions: e.g., *Maynard and Chen* [1975]. This led also *Goldstein et al.* [2002] to add an electric field component penetrating into the plasmasphere to obtain plasmaspheric shapes and positions fitting those observed on 24 May 2000, when a plasmaspheric shoulder was found in the EUV observations. In a subsequent study, *Goldstein et al.* [2003] included an additional E-field distribution related to subauroral polarization stream to obtain a better fit with plasmapause positions observed by EUV/IMAGE on 2 June 2001. The MHD simulations are essentially based on the postulate that the plasmapause coincides with the Last Closed Equipotential (LCE) of a stationary global magnetospheric electric field. When the magnetospheric electric field is not stationary, the plasmapause cannot be identified with the LCE of the time-dependent E-field, but may be assumed to correspond to a Last Closed Streamline (LCS). This is what will be assumed in the MHD simulations presented below. The second mechanism used below to predict the plasmapause positions and shapes is based on the mechanism of interchange reported in the book by *Lemaire and Gringauz* [1998]. These mechanisms are recalled and described in section 3.

[11] In section 4, we illustrate the plasmapause positions simulated for all three different electric fields models and with both kinds of mechanisms. The results are then compared with observations of EUV/IMAGE. Discussion and conclusion are given in the last section.

2. Models of Electric and Magnetic Fields

2.1. Volland-Stern's and Maynard-Chen's Convection Electric Field (VSMC)

[12] The Volland-Stern model [*Volland*, 1973; *Stern*, 1975] is a simple mathematical model where a uniform

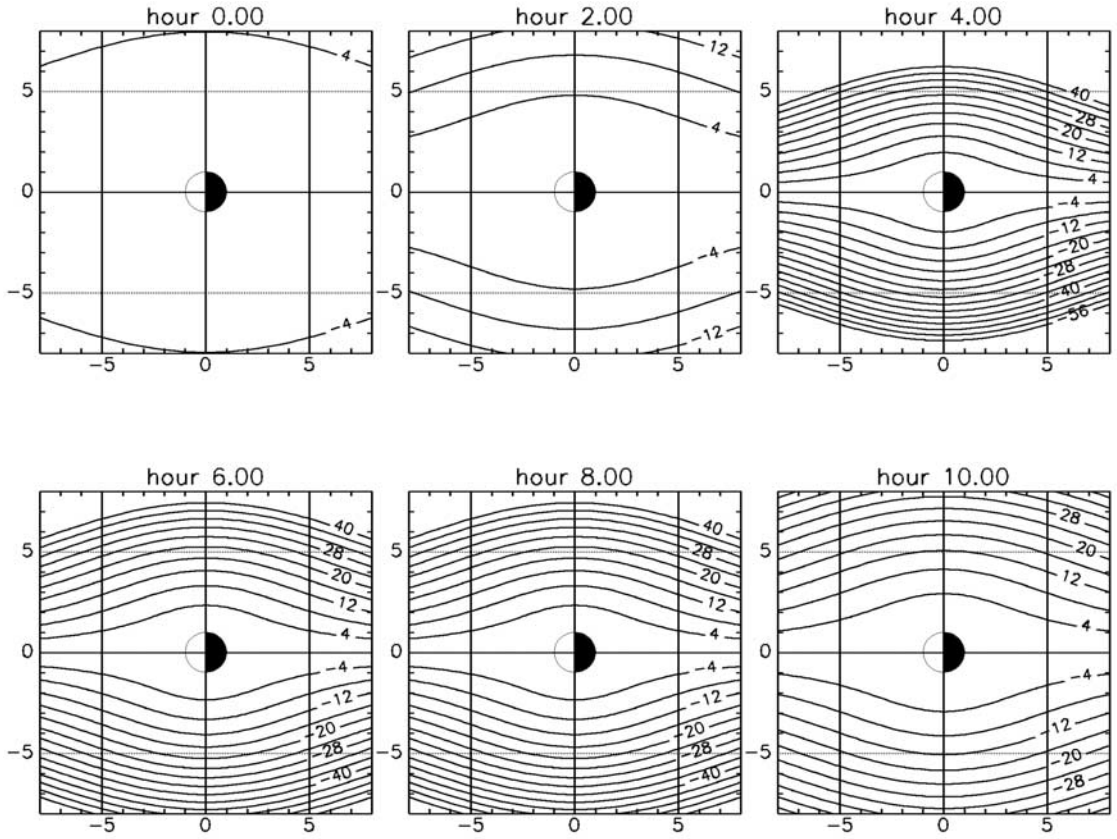

Figure 1. Equipotential contours of the convection electric field Volland-Stern on 28 October 2001 (without corotation electric field). The values of the potential (in kV) are given on the equipotential contours, which are drawn every 4 kV.

dawn-dusk convection electric potential distribution is applied across the magnetosphere. It has become very popular because of its simplicity and portability. In this model, there is no induced electric field resulting from time dependent magnetic field variations as can be envisaged during strong geomagnetic storms; the magnetospheric electric field derives from a scalar potential which, in a corotating frame of reference, is given by

$$\Phi = AR^2 \sin\phi$$

where R is the equatorial radial distance, ϕ is the azimuthal angle from noon and the Kp dependent factor $A = \frac{0.045}{(1-0.159Kp+0.0093Kp^2)^3}\left[\frac{kV}{R_E^2}\right]$ determines the convection electric field intensity.

[13] The Kp dependence of this empirical model was obtained by *Maynard and Chen* [1975] by adjusting the last closed equipotential (LCE) of the total E-field with plasmapause positions determined by OGO3 and OGO5 satellite observations; this is why this model has been given the acronym VSMC in the following. The Kp dependence is very sensitive especially at small values of Kp; the value of A varies from A = 45 V/R_E^2 for Kp = 0 to over 800 V/R_E^2 for Kp = 6.

[14] Figure 1 illustrates the equatorial contour maps of the equipotentials for the VSMC convection electric field every 2 h from 0:00 UT to 10:00 UT during the geomagnetic storm of 28 October 2001. To limit the effects of the artificial discontinuity appearing every 3 h in Kp index variation, we assume that a Kp increase (decrease) appears during the first hour (last half hour) of the 3 h range. A linear interpolated value of Kp is used during this variation. This evolution of Kp is illustrated by the blacked region in the top panels of the simulation figures (Figures 9 to 15). Because of this ''smoothed or filed down Kp variation'', the electric field varies more smoothly in our simulations. Figure 1 shows how the dawn-dusk electric field component is shielded close to the Earth and how it is assumed to change over this 10 h period. During this period of time, Kp increased from 1^- at 0:00 UT to 7^- at 05:00 UT, as illustrated in the top panels of Figure 9.

[15] In our simulations, this convection electric field is used with a centered dipolar magnetic field *B*. Indeed, this was the magnetic field assumed by *Maynard and Chen* [1975] to compute the MHD convection velocity: $(\vec{E} \times \vec{B})/B^2$.

2.2. McIlwain's E5D Convection Electric Field

[16] Another analytical representation of the magnetospheric convection electric potential was derived by *McIlwain* [1986] from electron and proton dynamical

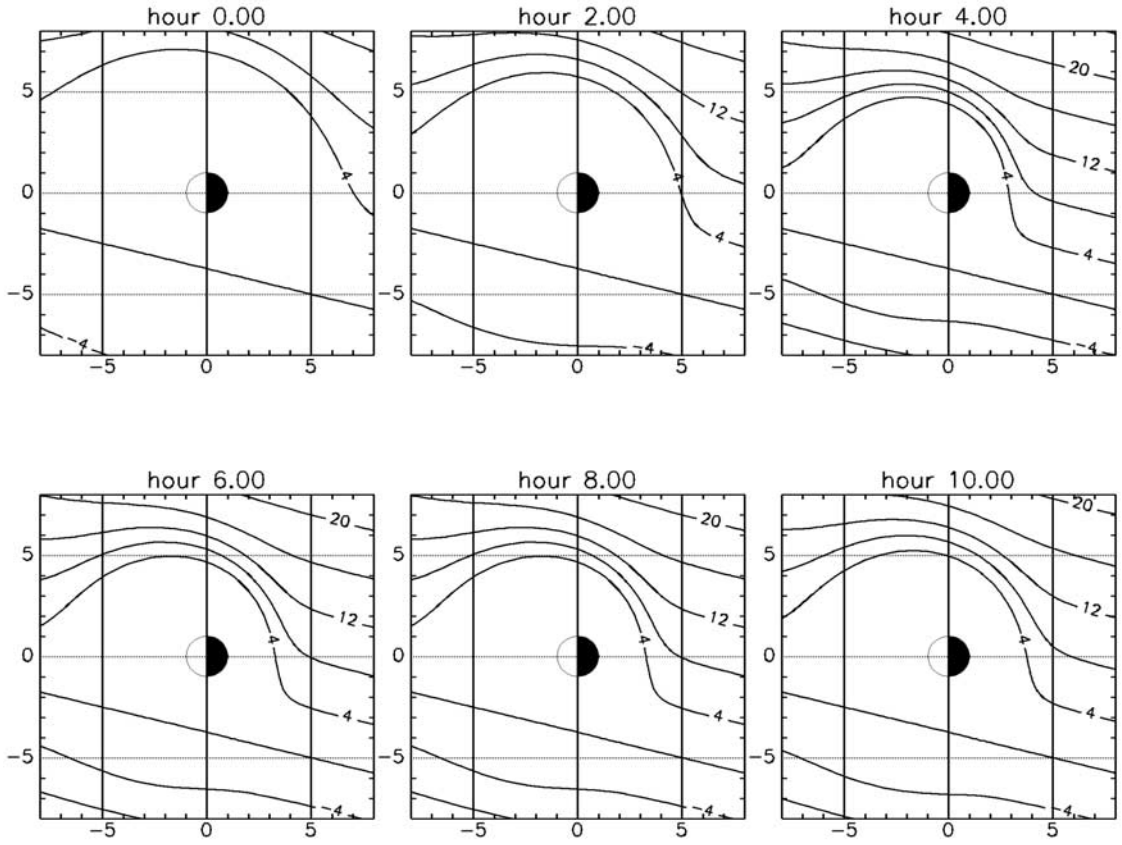

Figure 2. Equipotential map of the convection electric field E5D on 28 October 2001 (without corotation electric field). The values of the potential (in kV) are given on the equipotential contours, which are drawn every 4 kV.

spectra measured at geosynchronous orbit during the ATS-5 and ATS-6 missions:

$$\Phi = \{R(0.8\sin\phi + 0.2\cos\phi) + 3\}\left(1 + 0.3\frac{Kp}{1+0.1Kp}\right) \times \left(\frac{1}{1+\left(0.8*\frac{R_{ar}}{R}\right)^8}\right)$$

with $R_{ar} = 9.8 - 1.4\cos\phi + (-0.9 - 0.3\cos\phi)\frac{Kp}{1+0.1Kp}$.

[17] The E5D model depends also on the three-hourly geomagnetic activity index Kp. It has been found in past statistical studies that this index controls the observed positions of the plasmapause, when the level of geomagnetic activity changes. Note however that, unlike the VSMC model, the E5D model was not derived by adjusting its parameters to fit observed plasmapause positions, but was deduced from ATS-5 and ATS-6 particle flux measurements at geosynchronous altitude, precisely in the region where the plasmapause is formed. The E5D model was derived by fitting the observed positions of the injection boundary. The constants in the E5D electric potential model have been adjusted to fit the dynamical energy spectra in the range from 1 keV to 100 keV of electrons and protons injected following substorm events and observed in the equatorial region; according to McIlwain, this model is not necessarily reliable for Kp > 6, nor in the case of geomagnetic storms when rapidly changing electric field intensities are induced inside the magnetosphere.

[18] It should be emphasized that *McIlwain* [1986] did not develop his E5D model based on ATS-5 and ATS-6 observations collected during geomagnetic storm events, when Dst has large excursions. In principle, this model is designed to simulate the plasmapause formation and deformations during relatively steady state conditions following substorm injection events. Nevertheless, we will use it here during a geomagnetic storm with the caution that if the plasmapause positions predicted with this model would not fit adequately the observations during the geomagnetic storm, this may be due to the inadequacy of the E5D model to fit the actual electric field distribution during this period of time, and not necessarily to the inadequacy of the physical mechanism assumed to form the plasmapause.

[19] Figure 2 illustrates the equatorial equipotential contours for the E5D convection electric field model. These maps are shown every 2 h of UT from 0:00 to 10:00 during the geomagnetic storm of 28 October 2001. It clearly indicates the shielding of the dawn-dusk electric field component near the Earth in the dawn sector. A comparison with Figure 1 indicates that the E5D electric field model is less sensitive to changes of Kp than the VSMC model.

[20] To force a stronger Kp-variation, *Liemohn et al* [2001] rescaled the E5D model to match the cross-polar cap potential difference to other types of observations. This led them to define a "modified McIlwain" E-field model

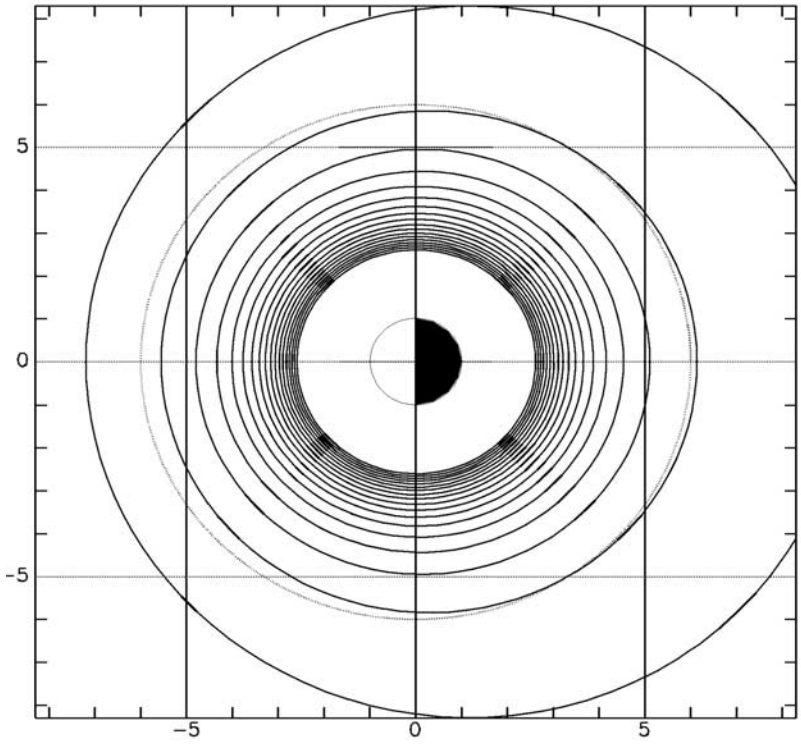

Figure 3. Magnetic field model M2. The dotted circle corresponds to L = 6; it exhibits the day-night asymmetry of the M2 model.

that should no more support ATS-5 and ATS-6 observations. In our simulations, we keep the original E5D model, as well as the associated M2 equatorial magnetic field model since both were derived from concomitant ATS-5 and ATS-6 observations.

[21] This M2 magnetic field model has a day-night asymmetry, and must be used in association with E5D to account for the actual day-night asymmetry of the convection velocities. Figure 3 illustrates the isocontours of the equatorial magnetic field intensity corresponding to the M2 model. Beyond five Earth radii, the deviations from a simple symmetric dipole become large especially in the nightside sector of the magnetosphere. Note that this B-field model does not depend on Dst nor on Kp unlike the model of *Tsyganenko and Stern* [1996]. Of course, this may be viewed as another limiting factor compromising its application to study the magnetic storm of 28 October 2001.

2.3. Weimer's Convection Electric Field

[22] Unlike the two previous E-field models, Weimer's model does not depend on the geomagnetic activity level Kp. The E-field model of *Weimer* [1996] is driven by solar wind parameters: interplanetary magnetic field magnitude, solar wind velocity and dipole tilt angle. It was derived from low altitude ionospheric convection velocity measurements at high latitudes. Unfortunately, these observations are collected far from the equatorial region where the plasmapause is formed during substorm events.

[23] Weimer electric potential [*Weimer*, 1996] is given by an expansion in spherical harmonics: $\Phi(\theta, \phi) = \sum_{l=0}^{Min(l,3)} (A_{lm} \cos m\phi + B_{lm} \sin m\phi) P_l^m (\cos \theta)$ where θ is a function of the geomagnetic colatitude, ϕ is the magnetic local time (MLT) and P_l^m are the associated Legendre functions. The coefficients A_{lm} and B_{lm} were derived by a least error fit from multiple satellite measurements of the ionospheric convection velocity.

[24] Figure 4 illustrates the equatorial contour maps of Weimer's convection electric potential every UT hour from 00:00 UT up to 11:00 UT during the geomagnetic event of 28 October 2001. These equatorial iso-contours of Weimer's equipotential are quite different from those illustrated in Figures 1 and 2. The shielding is less efficient in the dawn sector than at dusk unlike in Figure 2. From the distance between equipotential lines, it can also be seen that the electric field intensity is stronger than those illustrated in Figures 1 and 2. Moreover, Weimer's model depends on solar wind parameters varying over smaller timescales (60 min) and with larger amplitudes than the three-hourly index Kp controlling the VSMC and E5D models. Weimer's electric field intensity becomes especially strong in the dusk MLT sector at 4:00 UT at the beginning of the geomagnetic event while for the E5D model it is strongest in postmidnight sector (Figure 2) and in both the dawn and dusk sectors for the VSMC model (Figure 1).

[25] Weimer's electric field is used in association with the magnetic field model of *Tsyganenko and Stern* [1996] that is controlled by the following input parameters: solar wind pressure, Dst, the Y and Z components of the interplanetary magnetic field, and the geodipole tilt angle.

2.4. Corotation Electric Field

[26] To determine the total magnetospheric electric field in a non corotation frame of reference, the corotation

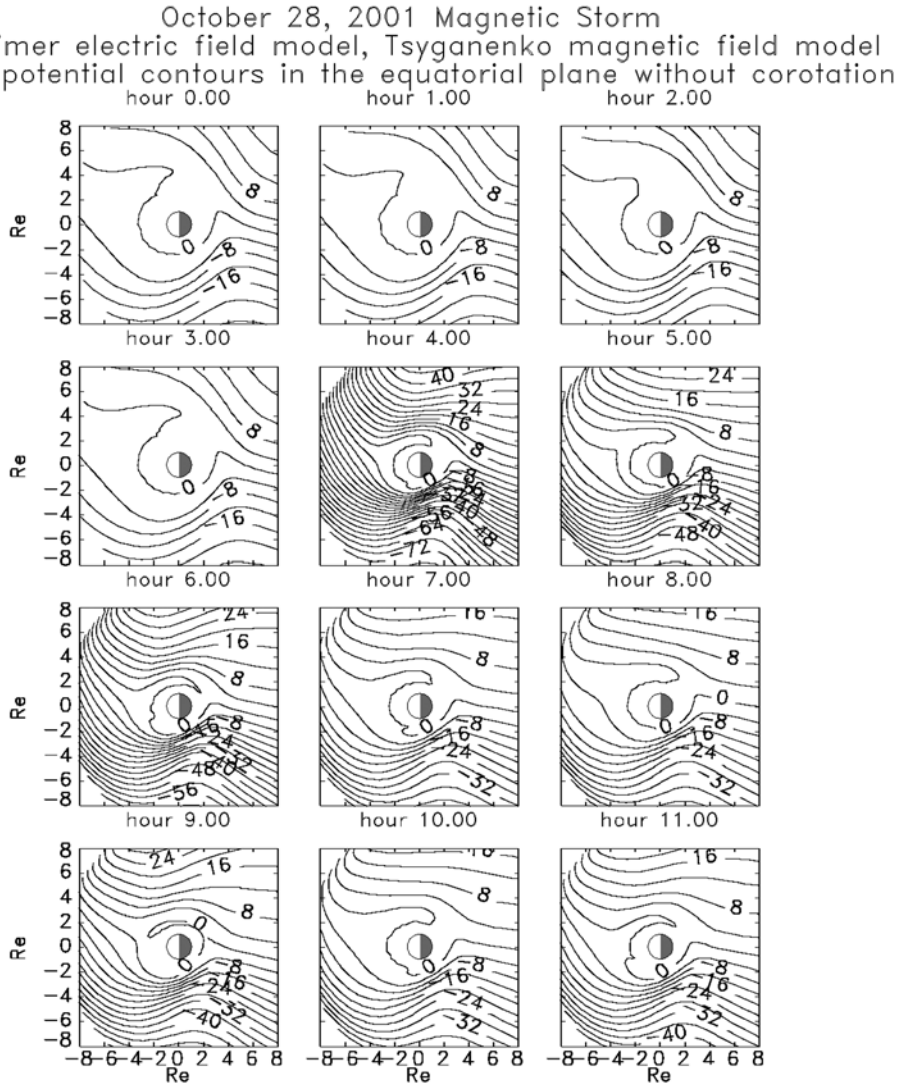

Figure 4. Equipotential map of the Weimer convection electric field dependent on solar wind conditions on 28 October 2001 (without corotation electric field). The values of the potential (in kV) are given on the equipotential contours, which are drawn every 4 kV.

electric field must be added to the convection electric field, postulating that these two E-field distributions could be superposed as in vacuum, despite the fact that the dielectric constant and permittivity of plasmas is much larger than that of free space. However, according to *Vasyliunas* [2001], this assumption is questionable, since any (external) electric field imposed from outside of a plasma system does directly determine the convection velocity deep inside this plasma system. It is the plasma bulk motion and the generalized Ohm's law that determine the E-field inside the magnetosphere; this internal E-field distribution does not necessarily coincide with a ''simple'' superposition of the ionospheric corotation electric field, and an external convection electric field induced by the solar wind. Indeed, due to the large dielectric constant, the latter does not penetrate inside the magnetosphere. Although such a simple superposition in a plasma (i.e., a highly dielectric medium) is not consistent with classical electrodynamics of dielectric material, it seems, nevertheless, to approximate the actual magnetospheric E-field distribution with mitigated success, at least this is what was generally considered within the community.

[27] The potential of the corotation electric field is given by:

$$\Phi = -\frac{92}{R}[kV].$$

[28] Note that it has been inferred from IMAGE observations that the azimuthal velocity of the plasmasphere is often slower (10% in average) than corotation in the outermost layers of the plasmasphere [*Burch et al.*, 2004]. This effect has been tentatively taken into account in some simulations by reducing the corotation potential by this ad hoc factor [*Pierrard*, 2006]. In the present work, however, we will consider that corotation is applicable, since all three

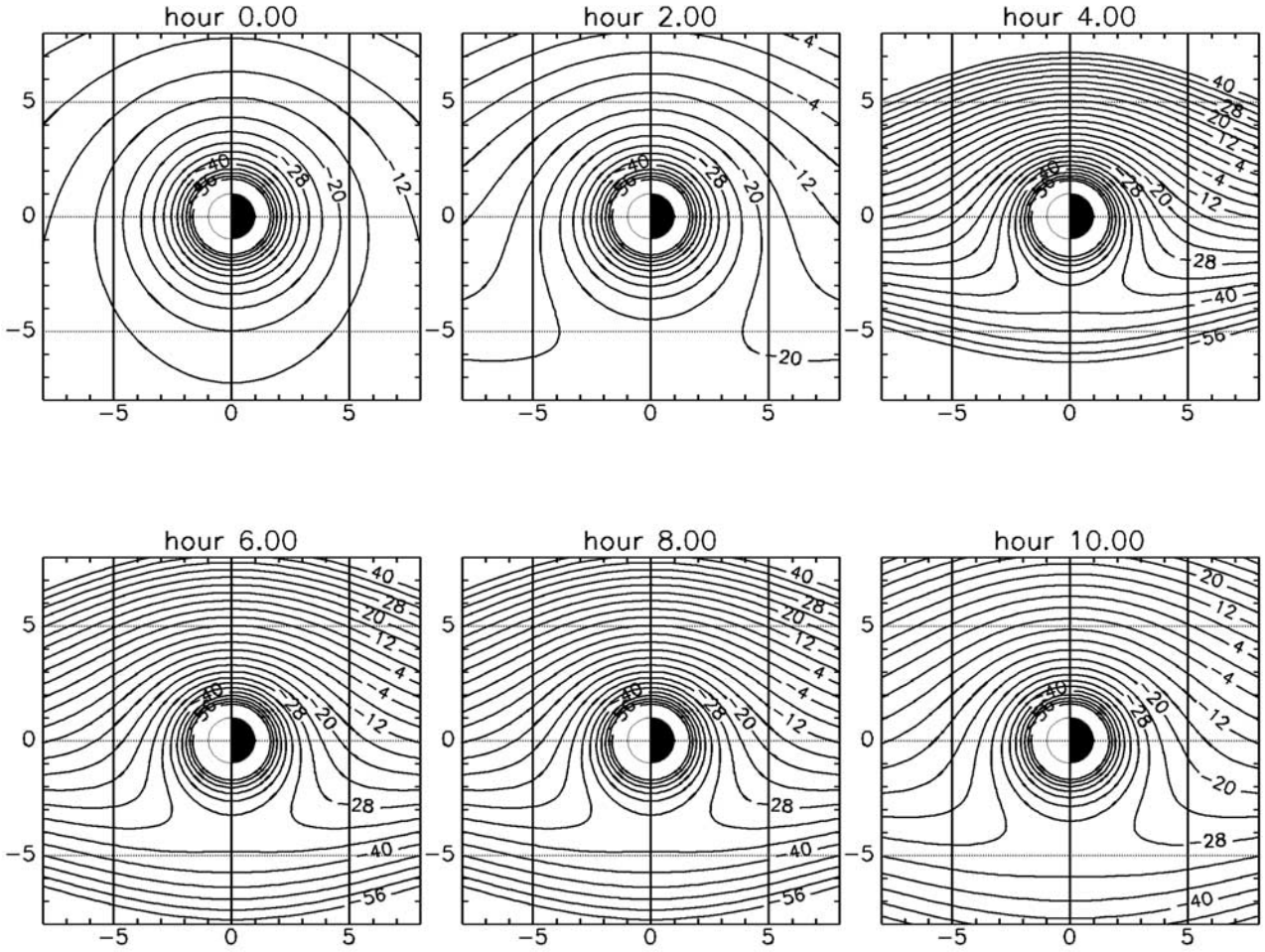

Figure 5. Equipotential map of the total electric field Volland-Stern on 28 October 2001. Same as Figure 1 but with corotation.

E-field models have been derived, originally, under such an assumption.

[29] In any case, the corotation electric field dominates near Earth, where the equipotential lines are closed and almost circular. This is evidenced in Figures 5, 6, and 7 showing the equatorial contour maps of the total electric potential in a noncorotating frame of reference, respectively for VSMC, E5D, and Weimer's convection electric field models every 2 h on 28 October 2001.

[30] Note the significant differences between all three models. The last closed equipotential has a stagnation point at 18:00 MLT in the dusk sector for VSMC and E5D models, while it is located at later MLT, in the postdusk local time sector, for Weimer's model. The LCE is everywhere closer to the Earth for the VSMC model than for the E5D one, for any value of the geomagnetic activity level $Kp > 1$.

[31] The E-field intensity increases to larger values for the Weimer model than for the two other models during this geomagnetic storm. Therefore the last closed equipotential penetrates closer to Earth for Weimer's model than for the two other models. For the VSMC model, the maximum E-field intensity is located in the morning sector (at 06:00 MLT). In the E5D model, the maximum intensity is in the postmidnight sector (around 2:00 MLT). Weimer's model also shows a maximum intensity in the postmidnight sector during the first hours preceding the geomagnetic storm similar to that displayed in the E5D model. During the storm main phase, this peak value moves closer to 06:00 MLT in both models.

[32] The evolution of the electric field (and magnetic field) in Weimer's model is controlled by the solar wind and geomagnetic parameters corresponding to 28 October 2001. Figure 8 shows the variation of the solar wind density of protons, the solar wind velocity and the Bx and By components of the interplanetary magnetic field obtained from SPENVIS (www.spenvis.oma.be) from 27 to 30 October 2001. The 3-hourly Kp, hourly disturbance storm time index Dst and Bz values are given in the three top panels of Figures 9, 10, 11, 12, 13, to 14. The smoothed Kp values used in the simulations are blacked up to the time corresponding to the displayed results, for instance 28 October 2001, 0h00 in Figure 9.

[33] Note that the 28 October 2001 storm is clearly associated to an increase of the solar wind velocity and density. Moreover, like most geomagnetic storms, it is initiated by a southward turning of the interplanetary magnetic field direction. The geomagnetic activity level

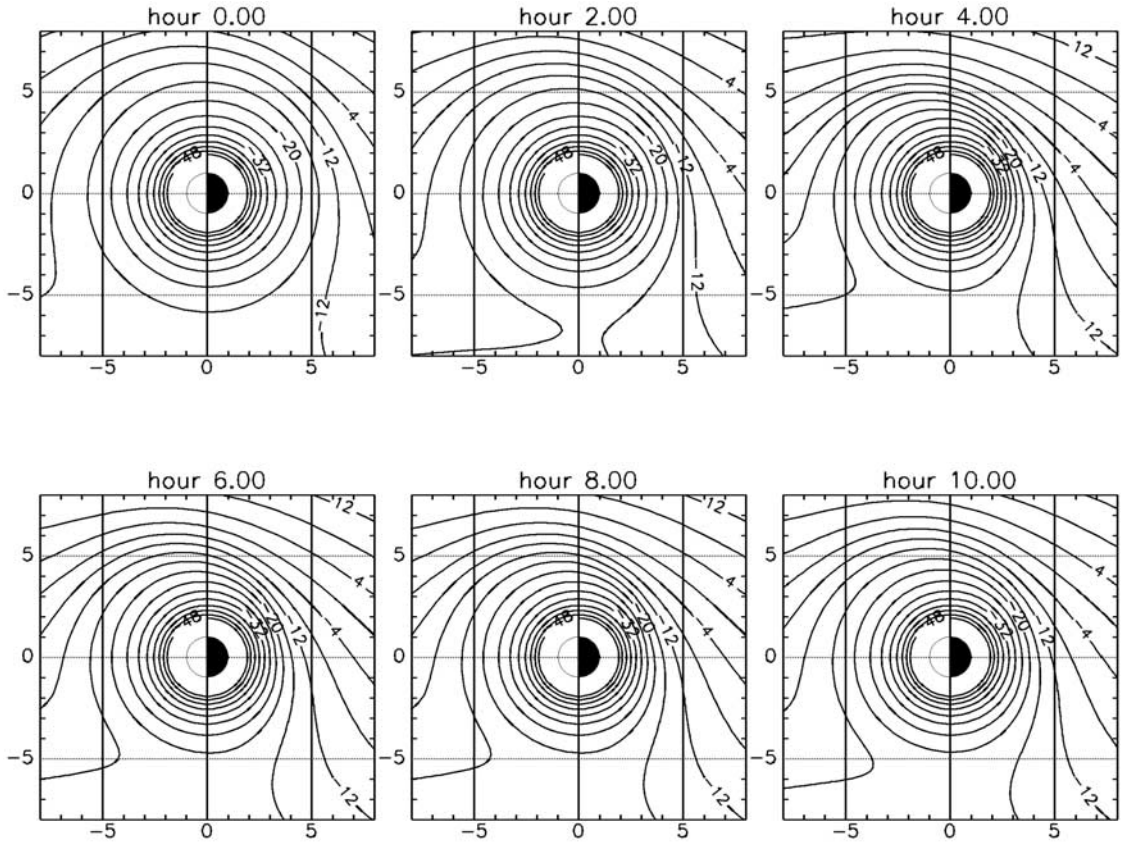

Figure 6. Equipotential map of the total electric field E5D on 28 October 2001. Same as Figure 2 but with corotation.

Kp index increases up to 7^-. The Dst index decreases by more than 150 nT.

3. Dynamical Simulations

3.1. Ideal MHD Simulations

[34] Different mechanisms have been proposed to form plasmaspheric "knee" or plasmapause. These mechanisms are described in detail in the book by *Lemaire and Gringauz* [1998]. The early theoretical MHD simulations by *Grebowsky* [1970] predicted that the evolution of the plasmapause is determined by the ideal MHD motion of the LCE at an arbitrarily chosen initial time t_0. In Grebowsky's early dynamical simulations, the plasmapause was assumed to coincide with the LCE surface at t_0. However, at any subsequent instant of time, the plasmapause did not coincide with the LCE of the changing convection E-field, unless the magnetospheric convection electric field would be independent of time.

[35] Our ideal MHD simulations differ from those of Grebowsky. They resemble more closely to those developed by *Rasmussen* [1992]. We launch plasma elements at 23:00 MLT, every 0.15 Re at radial distances ranging from 1.2 to 6 Re along an equatorial radius. The drift path of these ideal MHD plasma elements are calculated from $(\vec{E} \times \vec{B})/B^2$ where $\vec{E}$ and $\vec{B}$ are respectively the electric field and the magnetic field given by the adopted models. We let the plasma drift around the Earth for 24 h, and determine the last closed streamline (LCS) which is then used as the initial plasmapause position at time t_o. The ideal MHD drift path of all plasma elements proceeds until a time when EUV observations are available and can be used for comparison. Plasma elements are continuously launched from 23:00 MLT every 5 min, and tracked until they are deviated near the stagnation point, and are eventually lost at the magnetopause; we stop tracking any plasma element once it has completed one turn around the Earth. The equation of motion of each plasma element is integrated by a Runge-Kutta method with an adapted time step to satisfy a correct numerical accuracy; the equatorial positions of all plasma elements are stored every 5 min to map the deformations of the LCS as a result of Kp variations. For these ideal MHD simulations, the LCS is assumed to coincide with the plasmapause; it should be reminded that the LCS does not coincide at any time with the LCE of the convection electric field.

[36] In the regions close to the Earth where corotation is enforced, the plasmaspheric plasma is always highly coupled with that of the ionosphere. Since all flux tubes are on closed streamlines in this region, they are assumed to be completely full, and their densities are given by the empirical model of *Carpenter and Anderson* [1992]: $\log_{10} N_{eq} = -0.3145L + 3.9043$ where N_{eq} is the number density in electrons/cm^3 in the equatorial plane; it is independent of the local time angle, but it is a function of the McIlwain parameter L. Note also that it does not depend on the level of geomagnetic activity.

[37] The plasma elements located further away from the Earth are more significantly affected by the solar wind

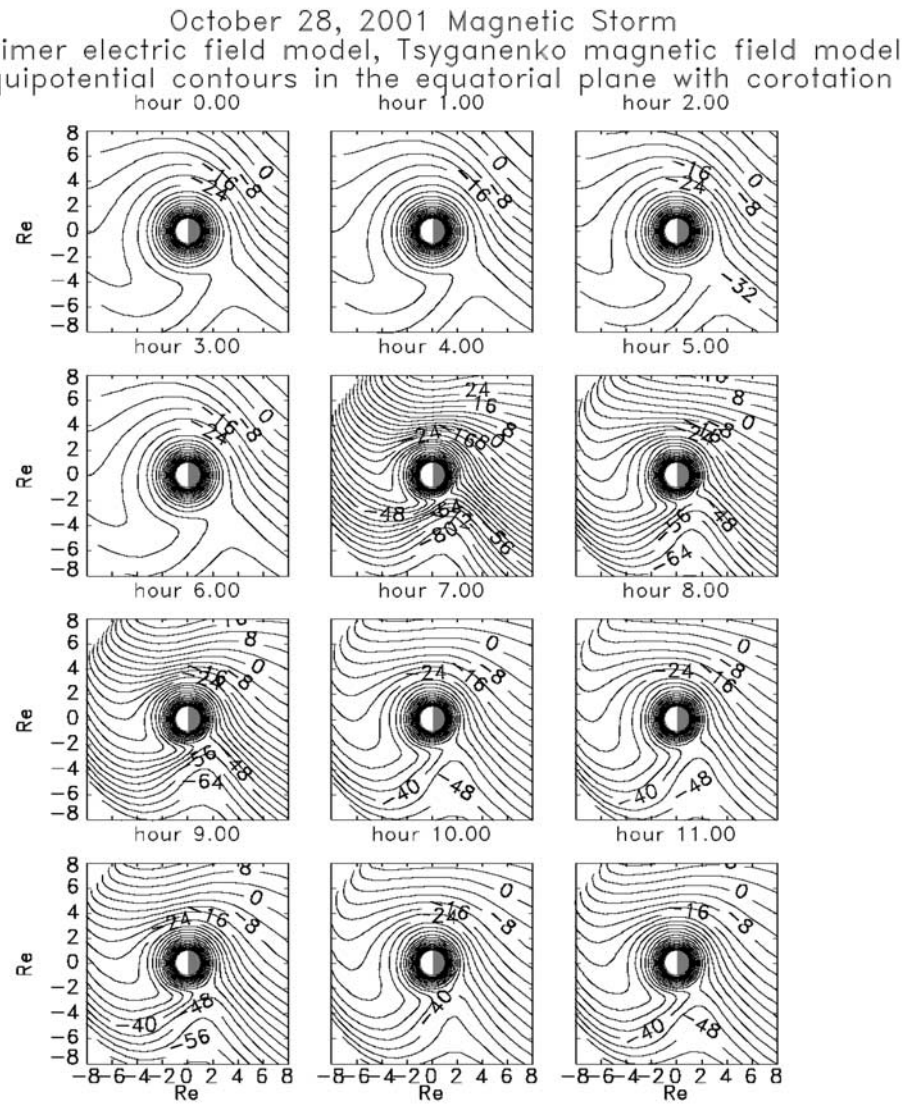

Figure 7. Equipotential map of the Weimer total electric field on 28 October 2001. Same as Figure 4 but with corotation.

induced magnetospheric convection. When the convection electric field is enhanced during periods of substorm injection events, the core of the plasmasphere where corotation dominates shrinks. The outer flux tubes beyond the last closed streamline (LCS) are eventually depleted in less than 24 h. When the convection electric field intensity decreases, the outermost flux tubes, which were depleted during the substorm, will gradually refill with cold plasma flowing up from the ionosphere. Quite long characteristic times (ranging from one to several days depending on the L values) are necessary to refill and saturate emptied flux tubes [*Lemaire and Gringauz*, 1998].

[38] Figure 9 (three upper panels) illustrates the results of these MHD simulations for 28 October 2001 at 00:00 UT for the three electric field models described above. In all the following figures, the upper left panels show the results for the E5D model; upper middle panels those for VSMC model, and upper right panels for Weimer's model. The symbols represent the plasma elements corresponding to the flux tube contents that were launched at 23:00 MLT 24 h before t_o. At small radial distances, the symbols form concentric circles corresponding to a contour of constant density content. At large radial distances, the contours of constant tube content become elongated in the predusk sector, indicating a decrease of the number density in this sector. Bottom left panel in Figure 9 corresponds to the result of the simulation based on the interchange mechanism for the formation of the plasmapause and E5D E-field model.

[39] We compare the successive positions of the plasmapause found with the MHD simulations assuming each point moves with the instantaneous $(\vec{E} \times \vec{B})/B^2$ drift velocity calculated with the three different E-field models: VSMC, E5D, and Weimer. Note that this convection velocity is never parallel to the equipotential lines of these models unless the E-field and B-field would both be stationary. Because of the continuously changing E-field distribution, the position of the LCS is a function of time. Let us recall

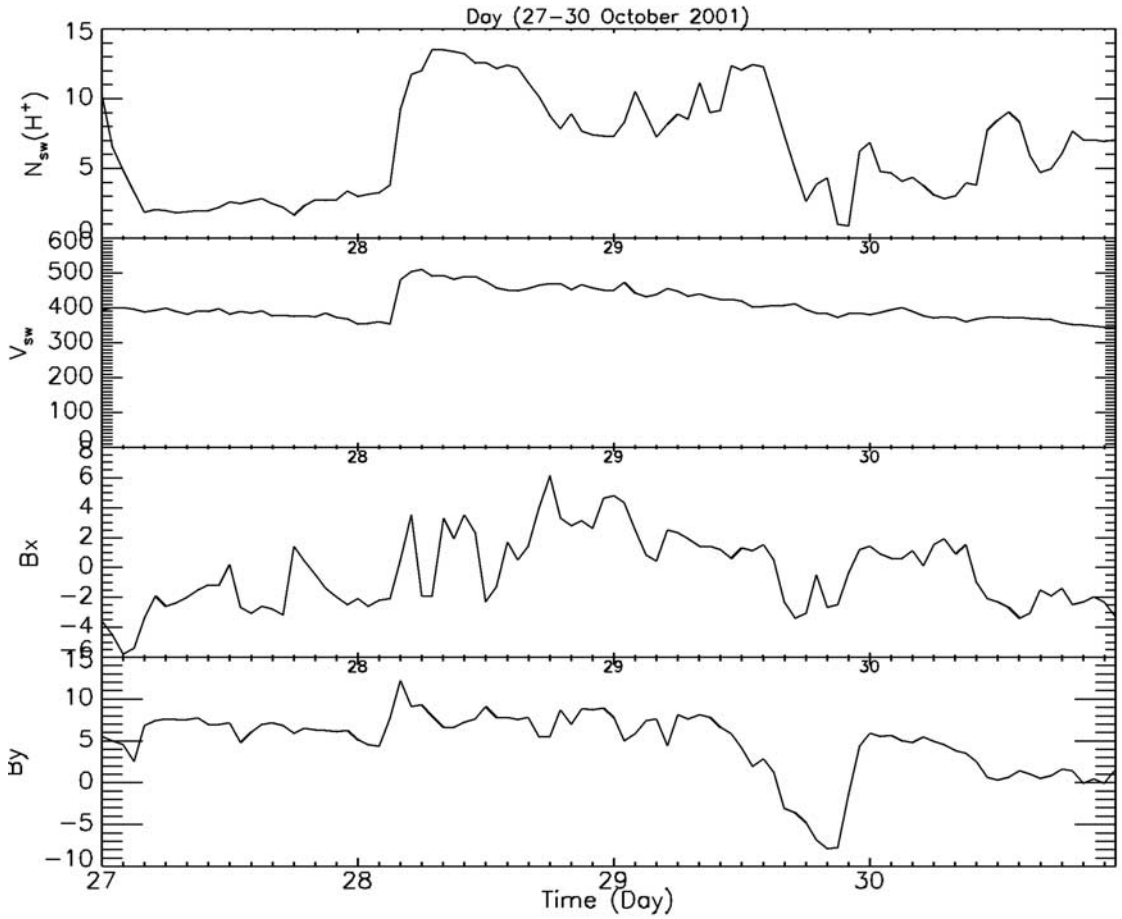

Figure 8. Variation of the solar wind density of protons, the solar wind velocity and the Bx and By component of the magnetic field from 27 to 30 October 2001.

that the LCS corresponds to the envelope of all drift paths that have not reached the magnetopause boundary during the previous 24 h. This is why it should be denoted LCS-24h. A different LCS could have been obtained if the closure time would have been 25 h, 2 d, 3d or 6 d as in the MHD simulations of *Chen and Wolf* [1972].

[40] The position of the LCS-24h found with our MHD simulations corresponds to the boundary where the number of plasma elements per unit area decreases sharply in Figures 9 to 15 (except at 23:00 MLT and beyond where new plasma elements are continuously launched every 5 min). If the plasmapause is identified with one of the last closed streamlines, it should be specified what is the closure time that has been adopted in the MHD simulations. This means that the location of the plasmapause, a physical boundary, would depend on the arbitrary choice of a closure time in any MHD simulation. This is clearly a conceptual limitation of the plasmapause with the LCS and even worse with the LCE.

[41] Figures 9 to 14 show that a plume is produced in the dusk sector during the magnetic storm in all three MHD simulations. This plume in the LCS-24h is similar to that observed by EUV/IMAGE after 18:00 UT.

[42] Figure 10 shows that at 04:30 UT, the LCS-24h has been pushed inward in the nightside region. Although the EUV observations show also an inward shift of the plasmapause near midnight, the overall shape of the plasmasphere is however very different from that of the LCS-24h obtained with the MHD simulations. While the LCS has rather smooth and regular shape, the actual plasmapause is much more indented and irregular. This can be a consequence of the rather poor time resolution of the Kp index controlling the E-field distributions. Since the magnetospheric E-field is changing over smaller timescale, the actual MLT variation of the LCS is expected to be more irregular than illustrated in Figures 10 to 14.

[43] Another important consequence of the shorter time variation of the E-field distribution, and of the associated plasma flow which must be quite variable, was pointed out by *Dungey* [1967] soon after the discovery of the sharpness of ''Carpenter's knee''. He wrote: ''Some tubes of high density (i.e., from inside the plasmasphere) should sometimes be swept out on the day side, and some tubes, after entering from the tail, should enter the inner region and, after a few days, should have intermediate values of density. It then seems rather surprising that the knee should be so sharp, but the variable model would predict a patchy density in the region near the knee and this could be the true state'' (sic). We share Dungey's early concern about the sharpness of a knee along the LCS. The short timescale variability of the magnetospheric plasma flow does not support the formation of sharp density gradients like those observed

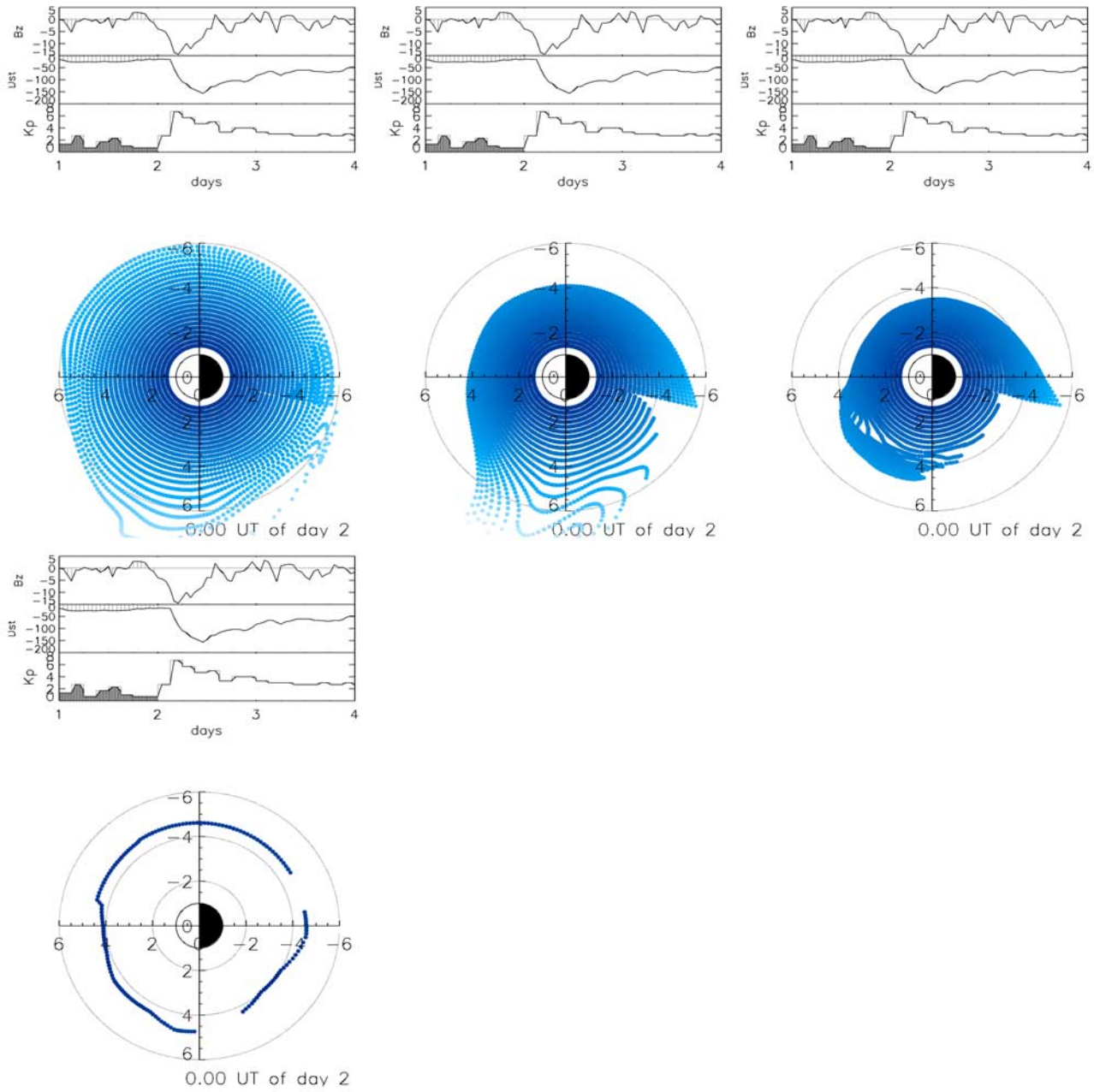

Figure 9. Initial plasmasphere determined with the MHD simulations using the E5D E-field model (upper left), MHD with Volland-Stern model (upper middle), MHD with Weimer model (upper right) and the plasmapause position predicted by instability mechanism with E5D (bottom left) on 28 October 2001 at 0:00 UT. The dotted circles correspond to L = 1, 2, 4, and 6. All these simulations started at 0:00 UT, 27 October 2001. The top of each panel shows the values of the northward component of the interplanetary magnetic field (Bz), the disturbance storm time index (Dst in nT), and the values of the geomagnetic index Kp during 3 d between 27 October 2001 and the end of 29 October 2001. The smoothed Kp value used in the simulations is blacked up to the universal time of the displayed result. No observations from EUV/IMAGE were available at that time.

soon after the peeling off of the plasmasphere which are associated with substorm events or inward motion of injection boundaries. However, the variability of the magnetospheric plasma flow may well account for the existence of the Plasmasphere Boundary Layer where *Carpenter and Lemaire* [2004] identified patchy plasma density irregularities.

[44] Note that the LCS corresponds in the MHD simulations of *Chen and Wolf* [1972] to the limit between magnetic flux tubes which have refilled for more than 24 h and those that have refilled for less than 24 h. If such a limit should correspond to the actual plasmapause, it must be admitted that the position of this physical boundary would depend on the choice of the refilling time which in our

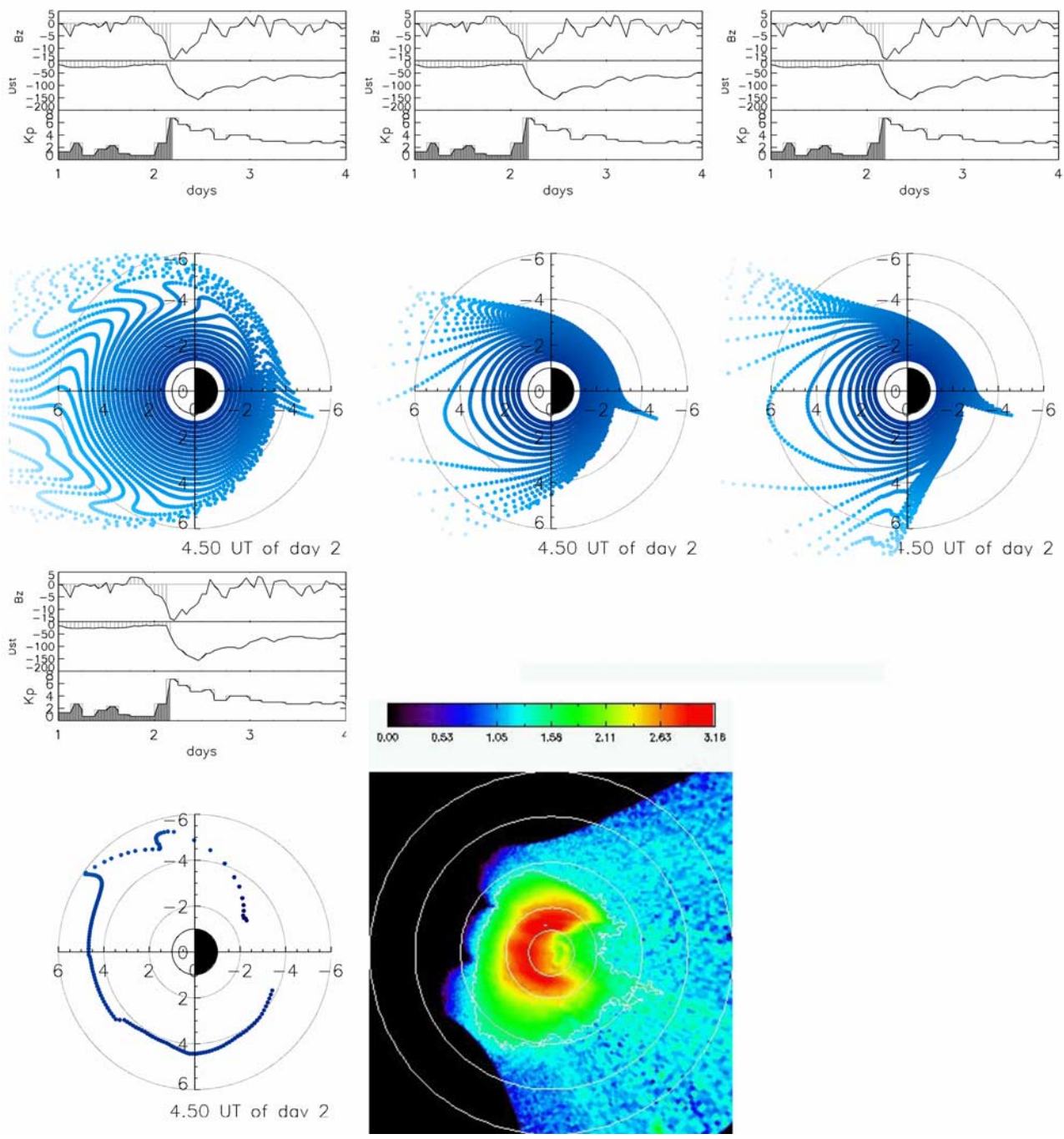

Figure 10. Results of the MHD E5D simulations (upper left), MHD VSMC (upper middle), MHD W (upper right), IC E5D (bottom left) at 4:30 UT, 28 October 2001. The EUV/IMAGE observation of the plasmasphere at 4:39 UT, projected in the geomagnetic equatorial plane, is illustrated in the bottom right. The view is from the North Pole with the Sun (local noon) to the left, like in the results of the simulations. The plasmapause is assumed to be the sharp edge where the brightness of 30.4 nm He^+ emissions drops drastically and is illustrated by the white line corresponding to a threshold equal to 40% of the maximum light intensity. The white circles correspond to L = 1, 2, 4, 6, and 8.

simulations was arbitrarily taken to be 24 h. In Chen and Wolf's MHD simulations different plasmapause locations were obtained when the refilling time was assumed to be 6 d, 5 d, 4 d, 3 d, 2 d or 24 h.

[45] This illustrates again the drastic limitation of identifying the plasmapause by any kind of MHD simulations whose results depend on an arbitrary choice of the closure time and a refilling time. Furthermore, the results of these MHD simulations rely also on the arbitrary choice of the initial time, t_0, when such simulations are assumed to start, and on the assumption of the density distributions in all flux tubes at this starting time.

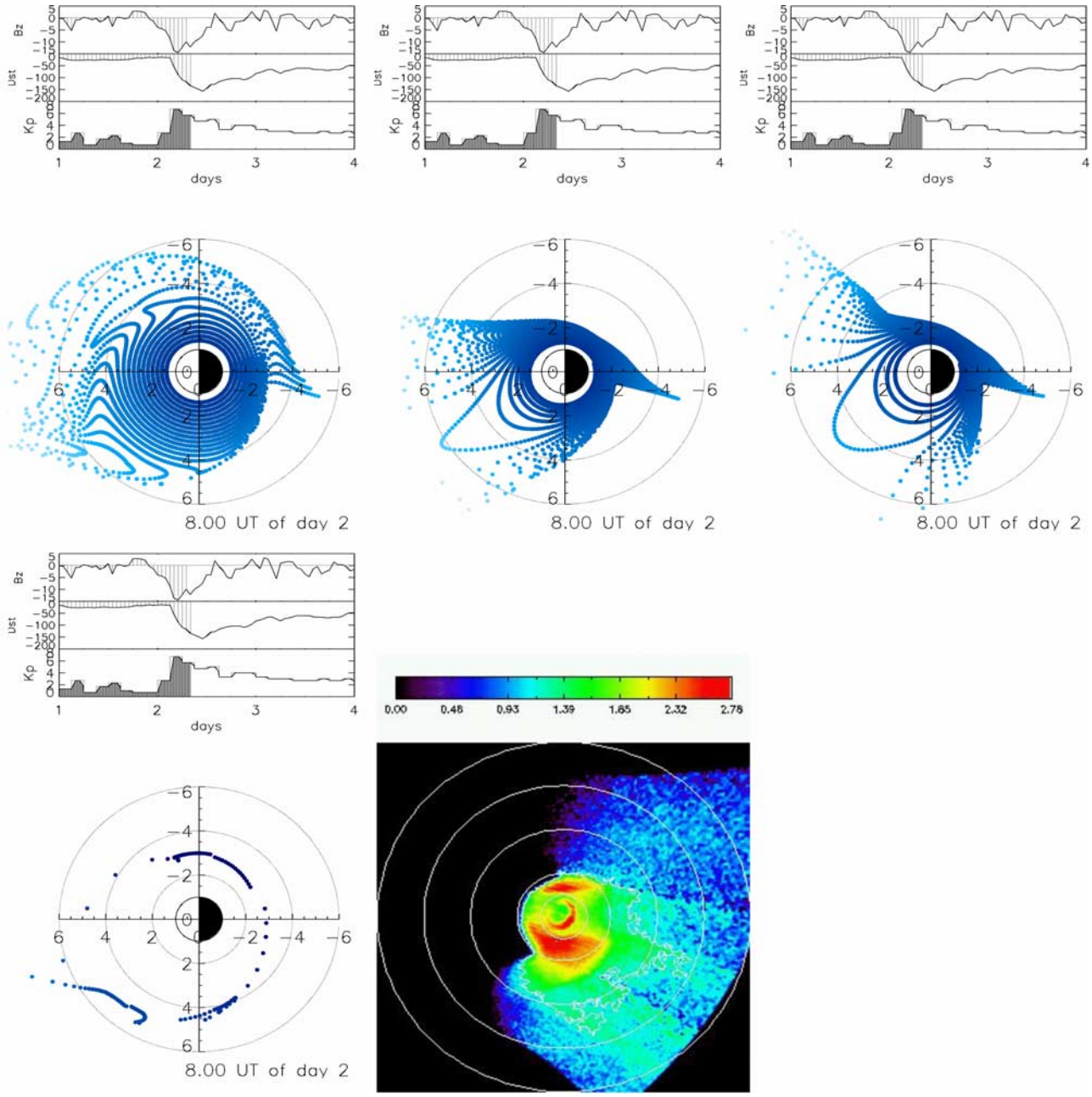

Figure 11. Results of the MHD E5D simulation (upper left), MHD VSMC (upper middle), MHD W (upper right), IC E5D (bottom left) at 8:00 UT, 28 October 2001. The EUV/IMAGE observation of the equatorial plasmapause position at 8:03 UT is illustrated in the bottom right panel.

3.2. Interchange Mechanism

[46] Another mechanism has also been proposed for the formation of the plasmapause: the interchange mechanism, illustrated by *Lemaire and Kowalkowski* [1981]. According to this mechanism, the plasma becomes unstable above a Zero Parallel Force (ZPF) surface where the parallel component of the gravitational plus centrifugal accelerations is equal to zero [*Lemaire*, 1985, 2001]. This occurs in the nightside local time sector during substorms and storms at an equatorial distance that depends on the distribution of the convection velocity. The plasmasphere is peeled off in this sector by the centrifugal effect which is enhanced when the convection velocity is enhanced beyond the inner edge of a substorm injection boundary. By this mechanism, a new plasmapause forms closer to the Earth than the LCS determined by the MHD simulations presented and discussed above. This mechanism has been used in numerical simulations performed by *Lemaire* [1985, 2000] and by *Pierrard and Lemaire* [2004]. The positions of the plasmapause predicted by this mechanism with the E5D model have been compared to observations of IMAGE for typical dates [*Pierrard and Cabrera*, 2005, 2006; *Pierrard*, 2006].

[47] In these non-MHD simulations based on the interchange mechanism, plasma holes with a density smaller than the background density are launched at 23:00 MLT in the equatorial plane. Because of the interchange motion,

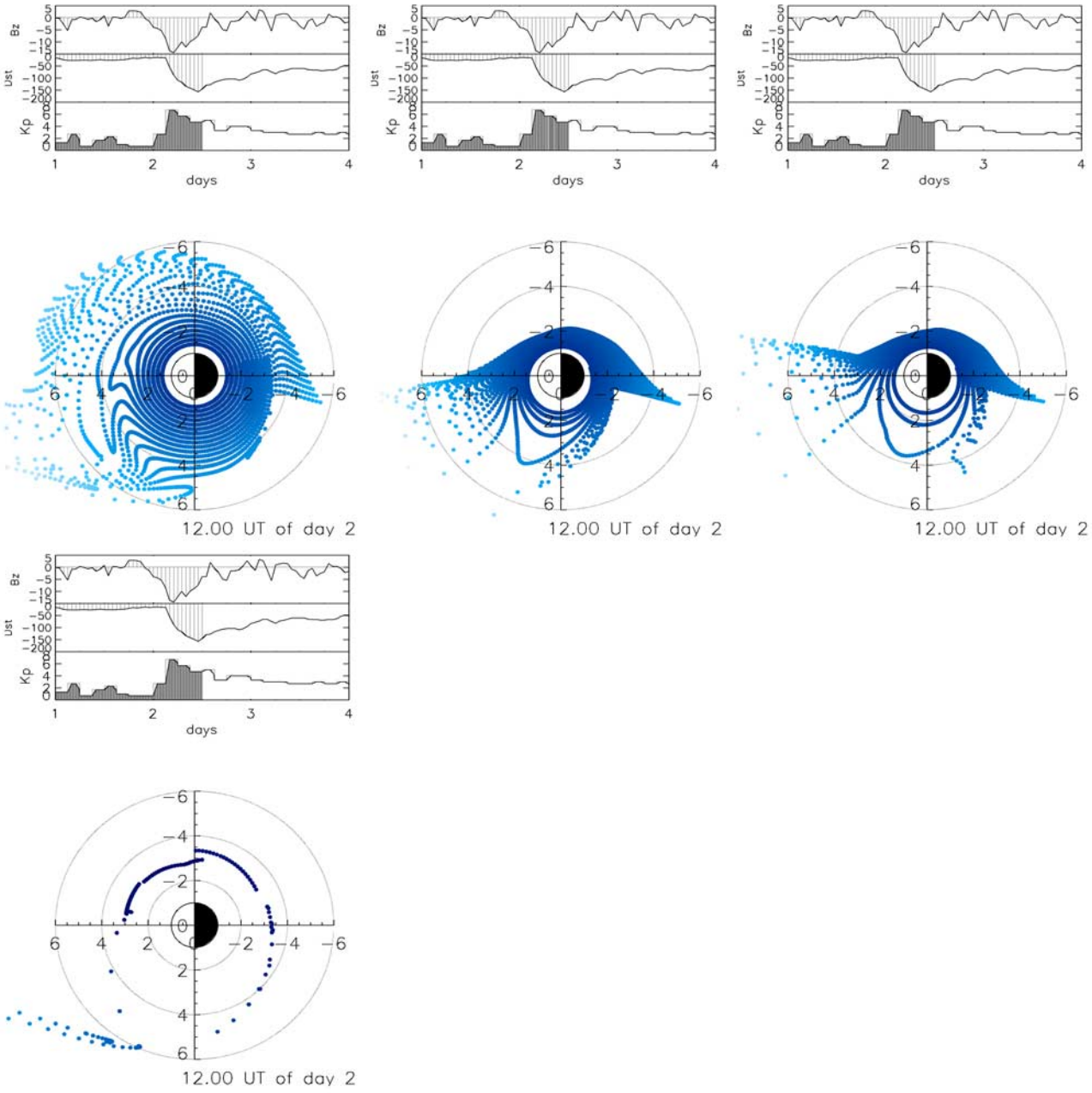

Figure 12. Results of the MHD E5D simulation (upper left), MHD VSMC (upper middle), MHD W (upper right), IC E5D (bottom) at 12:00 UT, 28 October 2001. No EUV/IMAGE observation is available at that time.

these holes drift ultimately toward an asymptotic trajectory where the radial component of the gravitational force and centrifugal force balance each other. This corresponds to the Zero Radial Force (ZRF) surface. However, the parallel components of these forces balance each other closer to the Earth along a virtual surface that *Lemaire* [1985] has called the Zero Parallel Force (ZPF) surface. It is assumed that the field aligned plasma distribution becomes convectively unstable along all flux tubes that traverse or are tangent to this virtual ZPF surface. In these flux tubes field aligned flow velocity is enhanced, and the plasma density is reduced due to its upward expansion. For a dipole magnetic field distribution the equatorial distance of the ZPF is $3^{2/3}$ time smaller than that of the ZRF surface. We assume that for the M2 magnetic field model the minimum equatorial distance of the ZPF surface is also approximately $3^{2/3}$ times smaller than that of the ZRF surface, as it is for a dipole B-field.

[48] To determine the plasmapause shape at t = 0 h on 28 October 2001, we run the interchange simulation between t = −24 h and t = 0 h. By this way, the position of the plasmapause obtained at t = 0 h is determined at all MLT angles by the interchange mechanism and by the history of the geomagnetic activity level during the previous 24 h. Note that the simulations could also be started by using an observed plasmapause position at the time t_0 like in the study of *Goldstein et al.* [2003]. This procedure would

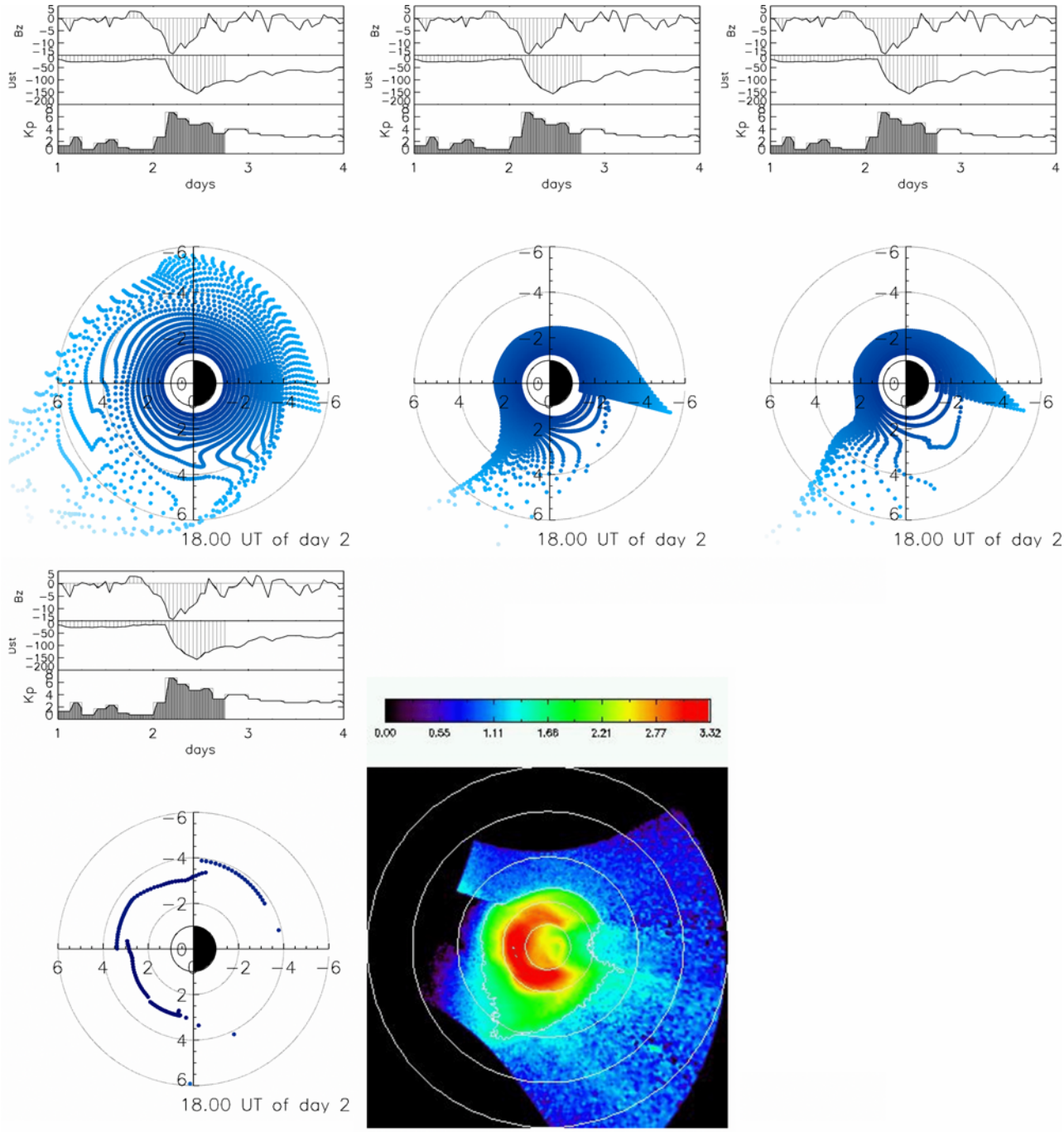

Figure 13. Results of the MHD E5D simulation (upper left), MHD VSMC (upper middle), MHD W (upper right), IC E5D (bottom left) at 18:00 UT, 28 October 2001. The EUV/IMAGE observation of the equatorial plasmapause position at 18:05 UT is illustrated in the bottom right panel.

of course favor the agreement between the results of the simulation and the observations at any subsequent times. Unfortunately, this procedure does not tell us about the physical mechanism that has formed this initial plasmapause; it may only be useful to test the appropriateness of the E-field models chosen in simulations, after the plasmapause had already formed.

[49] In the next section, we describe and compare the results obtained with the following series of simulations: MHD with the E5D model (MHD E5D), MHD with the Volland-Stern-Maynard-Chen model (MHD VSMC), MHD with the Weimer model (MHD W), and interchange with E5D model (IC E5D).

4. Discussion of the Results

4.1. Magnetic Storm of 28 October 2001

[50] Figures 9 to 14 illustrate the equatorial position of the plasmapause obtained with two different mechanisms for the formation of the plasmapause and three different

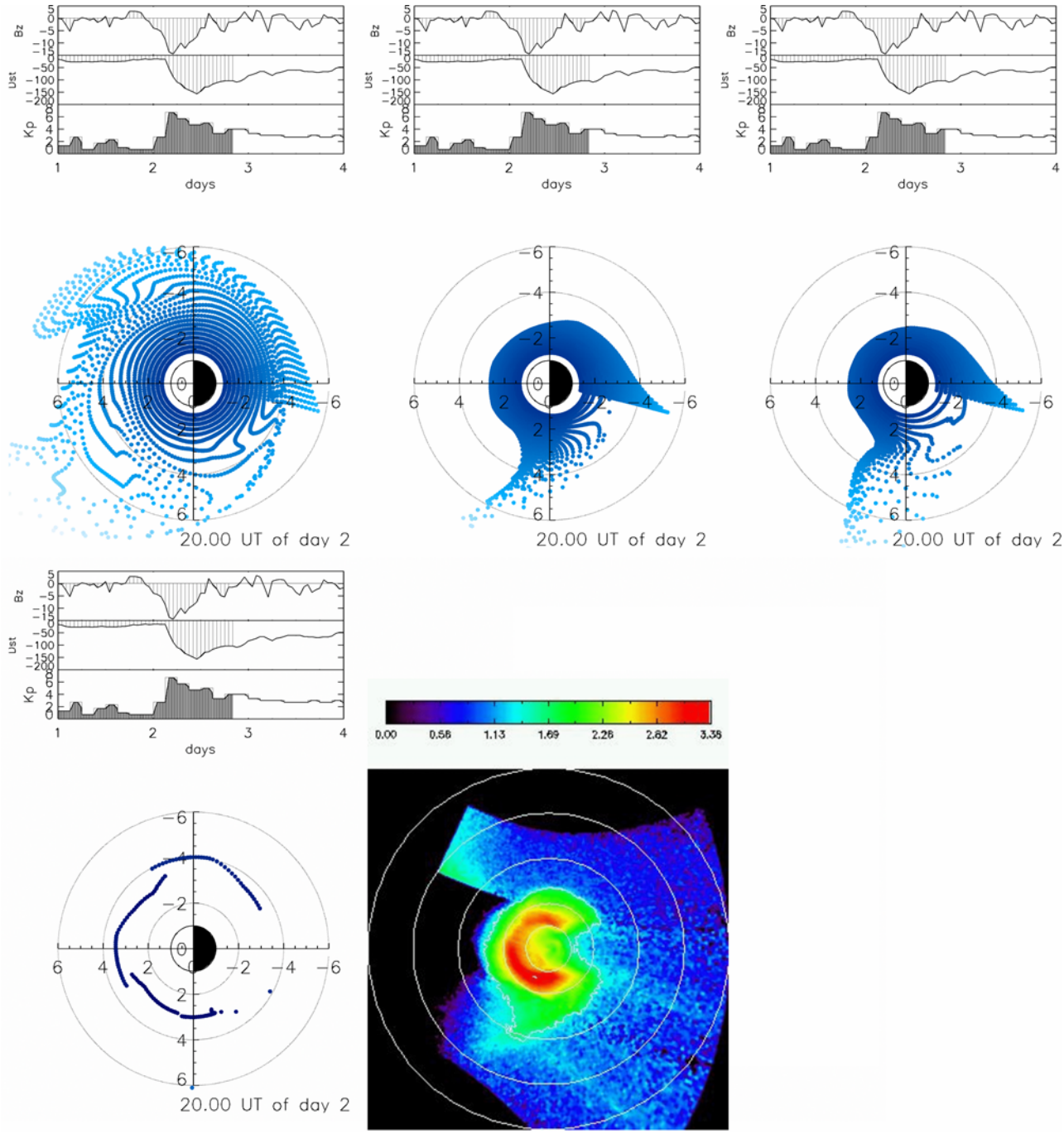

Figure 14. Results of MHD E5D simulations (upper left), MHD VSMC (upper middle), MHD W (upper right), IC E5D (bottom left) at 20:00 UT, 28 October 2001. The EUV/IMAGE observation of the equatorial plasmapause position at 19:58 UT is illustrated in the bottom right panel.

electric field models, respectively at 0:00, 4:30, 8:00, 12:00, 18:00, and 20:00 UT. The simulations correspond to MHD E5D (left upper panels), MHD VSMC (middle upper panels) and MHD W (right upper panels). The results obtained with the interchange mechanism and the E5D model are also presented in the left bottom panel of these graphs. The plasmapause found with the interchange mechanism is closer to Earth than with MHD simulations when a same E-field model is used. We do not provide simulations with interchange mechanism for the other electric field models since this would prohibitively increase the size of this paper without improving significantly its main results. Note also that the use of the interchange mechanism would not be physically significant in association with an E-field like the VSMC model which has been fitted in order to match the LCE with observed plasmapause positions.

[51] The top of each panel in Figures 9 to 14 illustrate the Kp and Dst indices and the northward component of the interplanetary magnetic field (Bz) from the beginning of 27 October 2001 to the end of 29 October 2001. At

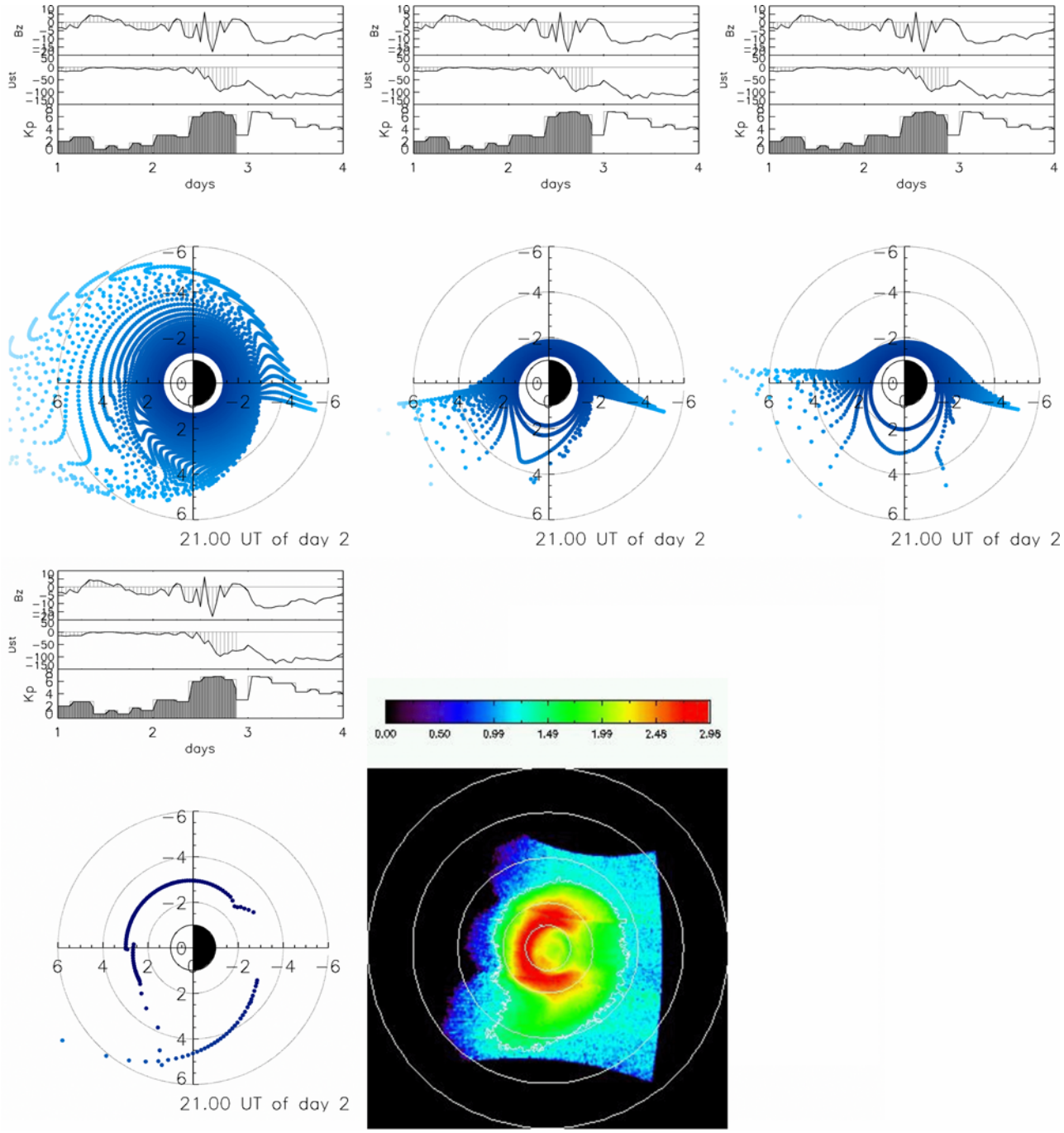

Figure 15. Results of MHD E5D simulations (upper left), MHD VSMC (upper middle), MHD W (upper right), IC E5D (bottom left) at 21:00 UT, after the magnetic storm of 17 April 2002. The EUV/IMAGE observation of the equatorial plasmapause position at 21:07 UT is illustrated in the bottom right panel.

00:00 UT, the level of geomagnetic activity is very low (Kp = 1^-) and increases to 7^- over the next 3 h when the main phase of the geomagnetic storm starts, i.e., when Dst begins a gradual drop, as shown on Figure 9.

[52] At 04:39, 08:03, 18:05, and 19:58 UT, there are exploitable observations from the EUV instrument since the orbit of the satellite IMAGE is close to its apogee. These images are presented in the bottom right panels of Figures 10, 11, 13, and 14, respectively. These observations are intensity maps of the 30.4 nm emissions of Helium ions integrated along the line of sight. They are projected in the geomagnetic equatorial plane in the SM coordinate system with the program XForm available at (ftp://euv.lpl.arizona.edu/pub/bavaro/unsupported/). This software tool enables to view the plasmapause cross section from over the North Pole like in our simulations. The bright arc close to the Earth is due to airglow of 58.4 nm neutral helium and oxygen ions. Its drop in intensity behind the Earth is caused by the Earth's shadow.

[53] The plasmasphere corresponds to the region surrounding the Earth and shown up mainly in green on the figures. The plasmapause is assumed to be the sharp edge where the brightness of 30.4 nm He^+ emissions drops drastically. This boundary is illustrated by a white line corresponding to a threshold equal to 40% of the maximum light intensity.

[54] Just before the storm, the MHD E5D simulation predicts at 00:00 UT a plasmasphere extending up to 6 Re. Since the dawn-dusk component of the two other convection electric fields (VMSC and Weimer) are stronger than that of the E5D model, the LCS is located closer to the Earth for these two other models: i.e., around 4 Re for the MHD VSMC, and even closer for the MHD W simulation. When the interchange mechanism is assumed to peel off the plasmasphere, the plasmapause at midnight LT is located around 4.5 Re with the E5D model; this is closer to Earth than the LCS simulation for this same E-field model. However, the plasmapause predicted by the IC E5D simulation is located at larger equatorial distances than the LCS for the two other E-field models. However, for a same E-field model, the minimum equatorial distance of the ZPF surface is generally smaller than that of the LCS.

[55] Note that the plasmasphere is almost circular at that time. Although the level of geomagnetic activity has been nearly constant and quite low during the previous 24 h, a bulge is present at 00:00 UT in the dusk sector in the MHD VSMC simulation. However, according to the EUV observations the plasmasphere is usually circular after prolonged quiet periods. Plasma tails or plumes are formed only during disturbed periods [*Pierrard and Cabrera*, 2005]. Unfortunately, no observations of EUV/IMAGE are available at 00:00 UT 28 October 2001, since the satellite was not close to its apogee at that time.

[56] At 04:30 UT as illustrated in Figure 10, the geomagnetic activity level Kp increases significantly and reaches a maximum Kp = 7^-. This increase of Kp is associated to a southward turning of the interplanetary magnetic field Bz, as well as a decrease of Dst index. The latter reaches a minimum of −157 nT at 11:00 UT. By that time, the convection electric field intensity has increased in all models so that the corresponding LCS-24h are less extended. Only the innermost flux tubes have a circular trajectory, while the more distant closed streamlines are highly skewed with a maximum radial distance in the postnoon sector. Beyond the LCS, the plasma elements are lost to the magnetosheath and are not any longer tracked in our MHD simulations. According to this MHD theory for the formation of the plasmapause, a more or less sharp knee is formed along the LCS-24h, wherein the streamlines have remained closed for at least 24 h.

[57] The LCS shrinks to about 3 Re in the night sector for all MHD simulations. A bulge is formed in the afternoon sector for all the simulations as a result of the enhancement of the dawn-dusk E-field component. Indeed, this enhancement of E-field in the dusk sector produces a sunward surge of plasma in this MLT sector. Note, however, the quite different shapes of the equatorial cross section of the LCS predicted by the various E-field models. The bulge in the LCS is the precursor of the plume that usually develops during geomagnetic storms and substorms.

[58] The interchange mechanism shown in the fourth panels produces much more irregular plasmapause shapes than the MHD simulations. From the fourth panel in Figure 10, it can be seen that the ZPF surface where the plasmasphere is peeled off in the postmidnight sector corresponds to an equatorial distance slightly beyond 2 Re. Despite the rather limited quality of the observations of IMAGE at the time of 04:30 UT, it can be seen that the plasmapause is located close to the Earth during this storm.

[59] At 08:00 UT, the Kp index is still high: Kp = 6^-. As illustrated in Figure 11, a plume is now clearly developed in all the simulations, with and without interchange. The plumes are located in the afternoon sector but have rather different shapes and experience quite different development depending on the adopted E-field model. The observation of EUV/IMAGE at 08:03 UT is very contaminated, but a plume can clearly be identified in the afternoon sector.

[60] With MHD VSMC and Weimer simulations, the plasmasphere is still smaller than with MHD E5D, due to their stronger dawn-dusk E-field intensity which implies a stagnation point rather close to Earth. The simulation of interchange with the E5D model, gives a position of the plasmapause which is rather close to that of the LCS of MHD E5D simulation.

[61] By 12:00 UT, the plume observed in the simulations has slightly rotated eastward as can be seen in Figure 12. No EUV observations are unfortunately available at that time. At 18:05 and 19:58 UT, EUV/IMAGE provides nice observations, and a plume is clearly visible in the afternoon/dusk region as illustrated in Figures 13 and 14. The results of the simulations are also shown for 18:00 and 20:00 UT. The longitudinal extent and MLT position of the plume is again slightly different in the different models. Note that by reducing arbitrarily the corotation velocity, a better agreement would be obtained. This kind of forcing has been avoided in the present work in order not to distort the original E-field models which have been derived without reducing the corotation electric field intensity. Note nevertheless that the velocity of the plasmasphere is observed to be generally slower than corotation [*Burch et al.*, 2004], which explains the faster rotation of the plume in the different simulations compared to the EUV observations.

[62] Similar plumes are often observed by EUV/IMAGE and CLUSTER after a significant increase of the geomagnetic activity level [*Darrouzet et al.*, 2006a, 2006b]. They are formed in the afternoon sector and then rotate eastward with the core of the plasmasphere. Other examples of IMAGE observations during quiet and disturbed periods that have been compared to results of simulations based on the interchange mechanism (IC E5D) have been presented by *Pierrard and Cabrera* [2005, 2006] and *Pierrard* [2006].

4.2. Magnetic Storm of 17 April 2002

[63] Figure 15 shows the results of similar simulations obtained during the geomagnetic storm of 17 April 2002. This case is particularly interesting since a global observational study of the dynamics of the plasmasphere, aurora, ring current and subauroral ionosphere was provided during this storm by *Goldstein et al.* [2005]. This is also the single event for which the effect of several electric field models on the position of the plasmapause has been also determined by *Liemohn et al.* [2004]. The E-field models tested in this

paper were (1) their modified E5D model rescaled to have a larger intensity than McIlwain's original version, (2) the Weimer model, and (3) a self consistent E-field determined by the authors. Thus it is interesting to compare the results of the present MHD simulations based on VSMC as well as on the original E5D model version with the results found by *Liemohn et al.* [2004] for the same event on 17 April 2002 with other E-fields models. Moreover, we also show the effect of the interchange mechanism on the positions, shape and evolution of the plasmapause during this magnetic storm.

[64] Figure 15 shows the results at 21:00 UT on 17-4-2002 obtained with the MHD simulations respectively for E5D, VSMC and Weimer models (three upper panels), as well as with interchange mechanism based on the E5D model (left bottom panel). A plume is again formed with all the electric field models. Its development is associated to the increase of the geomagnetic activity level up to $Kp = 7^+$. This increase of Kp is also associated with a southward turning of the interplanetary magnetic field, like during all geomagnetic storms. During the main phase, Dst decreases reaching a minimum of −105 nT on 17 April 2002 and even a lower value the day after. The plume is located approximately in the same MLT sector as in the observations of EUV. The MHD E5D simulation shows a plasmapause quite similar to that obtained with the rescaled E5D model used by Liemohn et al. The position of the plasmapause found by Liemohn et al. MHD simulation was in good agreement with the observations of EUV in the nightside, but it was too far from the Earth on the dayside. We obtain the same characteristics with the MHD E5D simulation.

[65] The MHD VSMC simulation corresponds better to the plasmapause observations on the dayside, but on the nightside, it is too close to the Earth. The MHD W simulation based on Weimer model gives also a plasmapause closer to the Earth than what is observed, especially on the nightside and on the morningside; these results are in agreement with the simulation published by Liemohn et al. where the Weimer convection E-field is also used.

[66] The simulation of the interchange mechanism with the E5D model gives results closer to the EUV observations than the MHD simulations with this same E5D electric field model. This does not imply, of course, that there is no need for better E-field model than E5D, nor is it a pleading for the mechanism of interchange, since any physical theory is necessarily an approximation and is therefore perfectible.

[67] While in general, interchange simulations with E5D model predict results that are in good agreement with the EUV observations during substorm events [*Pierrard and Cabrera*, 2005], we have seen here that such an agreement is more precarious during the geomagnetic storms examined in this paper. We attribute the lack of satisfactory results during geomagnetic storms to the lack of characterization of the E5D electric field model under this sort of geomagnetic disturbances. Indeed, this empirical E-field model was not designed to reproduce the magnetospheric convection electric field during geomagnetic storms, but only to model the dispersion of electrons and protons accelerated or injected into the magnetosphere following substorm events [*McIlwain*, 1986]. This lays the need to update and improve currently available empirical electric field models not only at ionospheric level but also at high altitudes in the Earth magnetosphere. Furthermore, nobody can argue that future alternative theories for the formation of the plasmapause will not be able to simulate the dynamics of the plasmasphere more accurately and offer predictions in closer agreement with observational reality.

5. Conclusions

[68] After brief descriptions of different electric fields models (the Volland-Stern-Maynard-Chen model VSMC, McIlwain's E5D model and the Weimer model), we first determined how the distribution of the equatorial equipotentials corresponding to these magnetospheric convection E-field models change during the geomagnetic storm of 28 October 2001. Their equipotentials in corotating and noncorotating frames of reference depend on the level geomagnetic activity; they are thus changing as a function of universal time since the geomagnetic activity indexes Kp and Dst are varying hour after hour.

[69] The radial and local time distributions of these equipotential contours have been displayed in Figures 1, 2, 4, 5, 6, and 7 for a set of times for which EUV observations are sometimes available. The E-field models are used in association with magnetic field models (VSMC/dipole, E5D/M2 model, and Weimer/Tsyganenko respectively), to calculate the convection velocity of cold plasma or the drift velocity of zero energy charged particles. The dipolar and M2 magnetic field models had been employed to design, respectively, the VSMC and E5D models from in situ satellite observations. In addition to their portability, these simple quasi-stationary E-field models have an expedient advantage: they depend only on one single parameter, the 3-hourly Kp geomagnetic activity index. This makes them user friendly and easy to implement in any numerical codes. Weimer E-field is more sophisticated: it depends on several solar wind parameters and varies with a higher time resolution. Nevertheless, it is based on low altitudes and high latitudes observations collected far from the equatorial region where the plasmapause is formed.

[70] Although all these empirical electric field models are based on observations (respectively, on OGO-3 & 5 satellites for VSMC, AST-5 & 6 satellites for E5D, and low altitude ionospheric convection velocity measurements at high latitudes for Weimer), they occur to be quite different from each other. Note that these models are averages and approximations of the actual field distributions at any particular instant of time, and at any particular place in the magnetosphere. Some of them were not designed to model magnetospheric electric fields in cases of rapidly changing magnetic field intensities: e.g., during geomagnetic storms when induction electric fields are generated on top of the electrostatic component approximated by these E-field models. For instance, the E5D model was essentially built to represent the E-field distribution immediately after a substorm injection event; furthermore, it was developed to represent the E-field in the region of geosynchronous orbit, only when the level of geomagnetic activity, denoted by the value of Kp, remains nearly constant and smaller than 6. McIlwain's electric field E5D was not developed under such circumstances as geomagnetic storms. However, taking into account these warnings and restrictions, it is interesting to note that the plasmapause position obtained with this E-field

model and the IC mechanism is in better agreement with the EUV observations during the geomagnetic storm of 17 April 2002 than the positions obtained with the other E-fields models and MHD simulations.

[71] Two mechanisms of plasmapause formation were also compared and confirm that the last-closed-streamline (LCS) of the MHD simulation is located beyond the plasmapause predicted by the interchange mechanism for the geomagnetic storm of 28 October 2001: the latter being thus generally closer to the Earth. A similar comparison with results obtained for the geomagnetic storm of 17 April 2002 leads to the same conclusions.

[72] The choice of the E-field model is crucial in the results of the simulations. Plumes develop during geomagnetic storms and substorms with all the various E-field models, but quite different shapes of the equatorial cross section of the LCS are predicted. It is quite clear that more detailed magnetospheric E-field models with higher time resolutions should be developed. In such future E-field models, the distribution of the equipotential surfaces should possibly be desynchronized: their evolution in the night side should not necessarily be synchronized with that in the dayside or at any other MLTs. Finally, it would be useful to model also the inductive electric field component in order to model more properly what happens during geomagnetic storms.

[73] Despite the better scores of the E5D electric field model and of the interchange scenario for the formation of the plasmapause found in many case studies, it must be admitted, however, that the equatorial cross section of the plasmapause as determined from the EUV observations during both geomagnetic storms, are not very well reproduced by none of the simulations presented above, not even when the Weimer electric field model is used instead of the E5D model. This leads us to conclude that none of the electrostatic field models is fully adapted to model the actual magnetospheric E-field distribution during geomagnetic storms (at least for those selected in the present study).

[74] Since previous simulations by *Pierrard and Lemaire* [2004] as well as by *Pierrard and Cabrera* [2005] based on the interchange mechanism and the E5D electric field model have shown that overall shapes of the plasmapause and its evolution does rather well explain the formation of plasmatails or plumes as well as shoulders following to substorm events, it may be speculated that during geomagnetic storms characterized by larger Dst variations, the time dependent electric field distribution has an induced component associated to the increase of southward magnetic field which is generated by the Ring Current during the main phase. A toroidal induced electric field of smaller intensity and of opposite direction is also expected during the recovery phase of geomagnetic storms. These toroidal induced electric fields cannot be represented as the gradient of a scalar electrostatic potential as most empirical magnetospheric E-field models used above. The effect of such additional time dependent and non curlfree electric field distribution on the plasmasphere and on the formation of the plasmapause, should be evaluated in detail.

[75] It is suggested here that such induced electric fields generated during geomagnetic storms are responsible for the lack of satisfactory agreement between the simulations presented in this study based on curlfree electric field models. We suggest that this effect should be examined in the future and included in forthcoming and more comprehensive theories for the formation of the plasmapause not only during substorm events but also even during geomagnetic storms with large Dst variations.

[76] Therefore this study points out the need to develop higher time resolution empirical models for the magnetospheric electrostatic field distribution like those developed for the geomagnetic field. It urges to take into account the effect of induced electric fields generated in the magnetosphere during geomagnetic storms with large Dst variations. An induced electric field model in the inner magnetosphere has to depend on Dst and on the Dst change rate (dDst/dt). Since it cannot be derived from the gradient of an electrostatic potential, this adds mathematical complexity to any future induced electric field model. However, it is only when such more detailed and comprehensive E-field models will be available in association with the time dependent empirical B-field models, that one might expect to test quantitatively and more definitely any of the existing and future theories for the formation of the plasmapause by comparing their theoretical predictions to observations like those of EUV.

[77] **Acknowledgments.** The authors thank the Belgian Science Policy office (SPP) for supporting this study. Support for George Khazanov was provided by the NASA LWS Program.

[78] Zuyin Pu thanks Iannis Dandouras and another reviewer for their assistance in evaluating this paper.

References

Albert, J. M. (2003), Evaluation of quasi-linear diffusion coefficients for EMIC waves in a multispecies plasma, *J. Geophys. Res.*, *108*(A6), 1249, doi:10.1029/2002JA009792.

Baker, D. N., S. G. Kanekal, X. Li, S. P. Monk, J. Goldstein, and J. L. Burch (2004), An extreme distortion of the Van Allen belt arising from the "Halloween" storm in 2003, *Nature*, *432*, 878, doi:10.1038/nature03116.

Boonsiriseth, A., R. M. Thorne, G. Lu, V. K. Jordanova, M. F. Thomsen, D. M. Thomsen, D. M. Ober, and A. J. Ridley (2001), A semiempirical equatorial mapping of AMIE convection electric potentials (MACEP) for the January 10, 1997, magnetic storm, *J. Geophys. Res.*, *106*, 12,903–12,917.

Brice, N. M. (1967), Bulk motion of the magnetosphere, *J. Geophys. Res.*, *72*, 5193–5211.

Burch, J. L., J. Goldstein, and B. R. Sandel (2004), Cause of plasmasphere corotation lag, *Geophys. Res. Lett.*, *31*, L05802, doi:10.1029/2003GL019164.

Carpenter, D. L., and R. R. Anderson (1992), An ISEE/whistler model of equatorial electron density in the magnetosphere, *J. Geophys. Res.*, *97*(A2), 1097–1108.

Carpenter, D. L., and J. Lemaire (2004), The plasmasphere boundary layer, *Ann. Geophys.*, *22*, 4291–4298.

Chen, A. J., and R. A. Wolf (1972), Effects on the plasmasphere of time-varying convection electric field, *Planet. Space Sci.*, *20*, 483–509.

Chen, M. W., M. Schulz, G. Lu, and L. R. Lyons (2003), Quasi-steady drift paths in a model magnetosphere with AMIE electric field: Implications for ring current formation, *J. Geophys. Res.*, *108*(A5), 1180, doi:10.1029/2002JA009584.

Cornwall, J. M., H. H. Hilton, and P. F. Mizera (1971), Observations of precipitating protons in the energy range 2.5 keV < E < 200 keV, *J. Geophys. Res.*, *76*, 5220.

Darrouzet, F., et al. (2006a), Plasmaspheric plumes: CLUSTER, IMAGE and simulations, in *Proceedings of the Cluster and Double Star Symposium*, *5th Anniversary of Cluster in Space*, pp. 1–6, ESA SP-598, ESTEC, Noordwijk, Netherlands.

Darrouzet, F., et al. (2006b), Analysis of plasmaspheric plumes: CLUSTER and IMAGE observations, *Ann. Geophys.*, *24*, 1737–1758.

Dungey, J. W. (1967), The theory of the quiet magnetosphere, in *Proceedings of the 1966 Symposium on Solar-Terrestrial Physics, Belgrade*, edited by J. W. King and W. S. Newman, pp. 91–106, Academic Press Inc., London.

Goldstein, J., R. W. Spiro, P. H. Reiff, R. A. Wolf, B. R. Sandel, J. W. Freeman, and R. L. Lambour (2002), IMF-driven overshielding electric field and the origin of the plasmaspheric shoulder of May 24, 2000, *Geophys. Res. Lett.*, *29*(16), 1819, doi:10.1029/2001GL014534.

Goldstein, J., B. R. Sandel, M. R. Hairston, and P. H. Reiff (2003), Control of plasmaspheric dynamics by both convection and subauroral polarization stream, *Geophys. Res. Lett.*, *30*(24), 2243, doi:10.1029/2003GL018390.

Goldstein, J., J. L. Burch, B. R. Sandel, S. B. Mende, P. C. son Brandt, and M. R. Hairston (2005), Coupled response of the inner magnetosphere and ionosphere on 17 April 2002, *J. Geophys. Res.*, *110*, A03205, doi:10.1029/2004JA010712.

Grebowsky, J. M. (1970), Model study of plasmapause motion, *J. Geophys. Res.*, *75*, 4329–4333.

Jordanova, V. K., L. M. Kistler, C. J. Farrugia, and R. B. Torbert (2001), Effects of inner magnetospheric convection on ring current dynamics, March 10–12, 1998, *J. Geophys. Res.*, *106*, 29,705–29,720.

Khazanov, G. V., M. W. Liemohn, T. S. Newman, M.-C. Fok, and A. J. Ridley (2004), Magnetospheric convection electric field dynamics and stormtime particle energization: Case study of the magnetic storm of 4 May 1998, *Ann. Geophys.*, *22*, 497–510.

Khazanov, G. V., K. Gamayunov, D. L. Gallagher, and J. U. Kozyra (2006), Self-consistent model of magnetospheric ring current and propagating electromagnetic ion cyclotron waves: Waves in multi-ion magnetosphere, *J. Geophys. Res.*, *111*, A10202, doi:10.1029/2006JA011833.

Khazanov, G. V., K. Gamayunov, D. L. Gallagher, J. U. Kozyra, and M. W. Liemohn (2007), Self-consistent ring current modeling with propagating electromagnetic ion cyclotron waves in the presence of heavy ions: 2. Ring current ion precipitation and wave induced thermal fluxes, *J. Geophys. Res.*, *112*, A04209, doi:10.1029/2006JA012033.

Lemaire, J. (1985), Frontiers of the plasmasphere, Thèse d'agrégation de l'Enseignement Supérieur, Jezierski ed., Aeronomica Acta A, No. 298, Cabay, Louvain-la-Neuve.

Lemaire, J. (2000), The formation of plasmaspheric tails, *Phys. Chem. Earth*, *25*, 9–17.

Lemaire, J. F. (2001), The formation of the light-ion trough and peeling off the plasmasphere, *J. Atmos. Sol. Terr. Phys.*, *63*, 1285–1291.

Lemaire, J. F., and K. I. Gringauz, with contributions from D. L. Carpenter and V. Bassolo (1998), *The Earth's Plasmasphere*, 350 pp., Cambridge Univ. Press, New York.

Lemaire, J., and L. Kowalkowski (1981), The role of plasma interchange motion for the formation of a plasmapause, *Planet. Space Sci.*, *29*(4), 469–478.

Liemohn, M. W., J. U. Kozyra, M. F. Thomsen, J. L. Roeder, G. Lu, J. E. Borovsky, and T. E. Cayton (2001), Dominant role of the asymmetric ring current in producing the stormtime Dst, *J. Geophys. Res.*, *106*(A6), 10,883–10,904.

Liemohn, M. W., A. J. Ridley, D. L. Gallagher, D. M. Ober, and J. U. Kozyra (2004), Dependence of plasmaspheric morphology on the electric field description during the recovery phase of the 17 April 2002 magnetic storm, *J. Geophys. Res.*, *109*, A03209, doi:10.1029/2003JA010304.

Maynard, N. C., and A. J. Chen (1975), Isolated cold plasma regions: Observations and their relation to possible production mechanisms, *J. Geophys. Res.*, *80*, 1009–1013.

McIlwain, C. E. (1986), A Kp dependent equatorial electric field model: The physics of thermal plasma in the magnetosphere, *Adv. Space Res.*, *6*(3), 187–197.

Pierrard, V. (2006), The dynamics of the plasmasphere, in *Space Science: New Research*, edited by N. S. Maravell, pp. 83–96, Nova Sci. Publ., New York.

Pierrard, V., and J. Cabrera (2005), Comparisons between EUV/IMAGE observations and numerical simulations of the plasmapause formation, *Ann. Geophys.*, *23*, 7, 2635–2646, SRef-ID: 1432-0576/ag/2005-23-2635.

Pierrard, V., and J. Cabrera (2006), Dynamical simulations of plasmapause deformations, *Space Sci. Rev.*, *122*, 1–4, 119–126, doi:10.1007/s11214-005-5670-8.

Pierrard, V., and J. Lemaire (2004), Development of shoulders and plumes in the frame of the interchange instability mechanism for plasmapause formation, *Geophys. Res. Lett.*, *31*, L05809, doi:10.1029/2003GL018919.

Rasmussen, C. E. (1992), The plasmasphere, in *Physics of Space Plasmas*, edited by T. Chang and J. R. Jasperse, pp. 279–302, Sci. Publ., Inc. Cambridge, Massachusetts.

Richmond, A. D., and Y. Kamide (1988), Mapping electrodynamic features of the high-latitude ionosphere from localized observations: 1. Technique, *J. Geophys. Res.*, *93*, 5741–5759.

Spasojevic, M., H. U. Frey, M. F. Thomsen, S. A. Fuselier, S. P. Gary, B. R. Sandel, and U. S. Inan (2004), The link between a detached subauroral protons arcs and a plasmaspheric plume, *Geophys. Res. Lett.*, *31*, L04803, doi:10.1029/2003GL018389.

Stern, D. P. (1975), The motion of a proton in the equatorial magnetosphere, *J. Geophys. Res.*, *80*, 595–599.

Summers, D., and R. M. Thorne (2003), Relativistic electron pitch-angle scattering by electromagnetic ion cyclotron waves during geomagnetic storms, *J. Geophys. Res.*, *108*(A4), 1143, doi:10.1029/2002JA009489.

Tsyganenko, N. A., and D. P. Stern (1996), Modeling the global magnetic field of the large-scale Birkeland current systems, *J. Geophys. Res.*, *101*, 27,187–27,198.

Vasyliunas, V. M. (2001), Electric field and plasma flow: What drives what?, *Geophys. Res. Lett.*, *28*, 2177–2180.

Volland, H. (1973), A semiempirical model of large-scale magnetospheric electric fields, *J. Geophys. Res.*, *78*, 171–180.

Weimer, D. R. (1996), A flexible, IMF dependent model of high-latitude electric potentials having "space weather" applications, *Geophys. Res. Lett.*, *23*, 2549–2552.

J. Cabrera, Center for Space Radiations, Université Catholique de Louvain, 2 chemin du cyclotron, 1348 Louvain-La-Neuve, Belgium.

G. V. Khazanov, NASA Marshall Space Flight Center, Science and Exploration Office, VP62, National Space Science and Technology Center, 320 Sparkman Drive, Huntsville, AL 35805, USA.

J. Lemaire and V. Pierrard, Belgian Institute for Space Aeronomy, 3 avenue Circulaire, B-1180 Brussels, Belgium. (viviane.pierrard@oma.be)